CGC/saturation approach for high energy soft interactions: v_2 in proton-proton collisions

E. Gotsman,[1,*] E. Levin,[1,2,†] U. Maor,[1,‡] and S. Tapia[2,§]

[1] *Department of Particle Physics, School of Physics and Astronomy, Raymond and Beverly Sackler Faculty of Exact Science, Tel Aviv University, Tel Aviv, 69978, Israel*

[2] *Departemento de Física, Universidad Técnica Federico Santa María, and Centro Científico-Tecnológico de Valparaíso, Avda. Espana 1680, Casilla 110-V, Valparaíso, Chile*

(Dated: March 16, 2016)

In this paper we continue our program to construct a model for high energy soft interactions, based on the CGC/saturation approach. We demonstrate that in our model which describes diffractive physics as well as multi-particle production at high energy, the density variation mechanism leads to the value of v_2 which is about $60\% \div 70\%$ of the measured v_2. Bearing in mind that in CGC/saturation approach there are two other mechanisms present: Bose enhancement in the wave function and local anisotropy, we believe that the azimuthal long range rapidity correlations in proton-proton collisions stem from the CGC/saturation physics, and not from quark-gluon plasma production.

PACS numbers: 12.38.-t,24.85.+p,25.75.-q

arXiv:1603.02143v1 [hep-ph] 7 Mar 2016

INTRODUCTION

The large body of experimental data on soft interactions at high energy[1–9], presently, cannot be described in terms of theoretical high energy QCD (see [10] for a review).

In this paper we continue our effort[11–15] to comprehend such interactions, by constructing a model that incorporates the advantages of two theoretical approaches to high energy QCD: the CGC/saturation approach [16–22] and the BFKL Pomeron calculus[16, 23–32] . Both provide an effective theory of QCD at high energies. However, the interpretation of processes at high energy appear quite different in each, since they have different structural elements.

The CGC/saturation approach describes the high energy interactions in terms of colorless dipoles, their density, distribution over impact parameters, evolution in energy and so on. Such a description appears quite natural in perturbative QCD, and can be easily applied to multi-particle production at high energy. In this approach a new saturation scale Q_s occurs which is much larger than the soft scale, and the description of the production of quarks and gluons can be attained theoretically, in an economical way. The transition from quarks and gluons to hadrons, has to be handled phenomenologically using data from hard processes. This approach leads to a good description of the experimental data on inclusive production, and the observation of some regularities in the data, such as geometric scaling behaviour[33–38].

BFKL Pomeron calculus which deals with BFKL Pomerons and their interactions, is similar to the old Reggeon theory [39], and is suitable for describing diffractive physics and correlations in multi-particle production, as we can use the Mueller diagram technique[40]. The relation between these two approaches has not yet been established, but they are equivalent[31] for rapidities ($\ln(s/s_0)$), such that

$$Y \leq \frac{2}{\Delta_{\rm BFKL}} \ln\left(\frac{1}{\Delta^2_{\rm BFKL}}\right) \tag{1}$$

where $\Delta_{\rm BFKL}$ denotes the intercept of the BFKL Pomeron. As we have discussed [11], the parameters of our model are such that for $Y \leq 36$, we can trust our approach, based on the BFKL Pomeron calculus.

This paper is the next step in our program to construct a model for high energy soft scattering, based on an analytical calculation, without using Monte Carlo simulations.

One of the most intriguing experimental observations made at the LHC and RHIC, is the same pattern of azimuthal angle correlations in the three types of interactions: hadron-hadron, hadron-nucleus and nucleus-nucleus collisions. In all three reactions, correlations in the events with large density of produced particles, are observed between two charged hadrons, which are separated by the large values of rapidity. [1, 41–46].

We believe that the results of these experiments provide strong evidence, that the underlying physics is the same for all three reactions, and is due the high density partonic state that has been produced at high energies, in all three reactions. Due to causality arguments[47] two hadrons with large difference in rapidity between them, could only correlate at the early stage of the collision and, therefore, we expect that the correlations between two particles with

large rapidity difference (at least the correlations in rapidity) are due to the partonic state with large parton density. The parton (gluon) density is governed in QCD by the CGC/saturation non-linear equations and therefore, the CGC approach is the appropriate tool to study these correlations.

Unlike, the rapidity correlations at large values of the rapidity difference, which stem from the initial state interactions, the azimuthal angle correlations can originate from the collective flow in the final state [48]. Nevertheless, in this paper we would like to analyze the same mechanism for both correlations: i.e. the initial state interaction in the CGC phase of QCD. However, even in the framework of the saturation/CGC approach, we presently are not able to propose a unique mechanism for the azimuthal angle correlations. At the moment three sources for the azimuthal angle correlation have been suggested: [74] Bose enhancement in the wave function[50], local anisotropy[51, 52] and density variation [36]. We cite only a restricted number of papers for each approach. The reader can find more references, and more ideas on the origin of the correlations in the review papers Refs.[52–58].

The goal of this paper is to study in more detail the density variation mechanism proposed in Ref.[36]. In this approach, both rapidity and azimuthal angle correlations originate from two gluons production from two parton showers.

This process can be calculated using Mueller diagrams [40] (see Fig. 2-a). The difference between rapidity and azimuthal angle correlations is only in the form of the Mueller vertices in this figure. For rapidity correlations, such vertices can be considered as being independent of Q_T, while for the azimuthal angle correlation, this vertex is proportional to $\left(\boldsymbol{Q}_T \cdot p_{1,\perp}\right)^2$ or $\left(\boldsymbol{Q}_T \cdot p_{2,\perp}\right)^2$. The integration over the direction of $\boldsymbol{Q}_T$ leads to the term $\left(\boldsymbol{p}_{1,\perp} \cdot \boldsymbol{p}_{2\perp}\right)^2$, which is proportional to $\cos 2\varphi$, resulting in azimuthal angle correlations. The strength of the term $\cos 2\varphi$ is proportional to $\langle Q_T^2 \rangle^2$, where averaging is over the wave function of the one parton shower, which is described by the BFKL Pomeron. In other words since $\boldsymbol{Q}_T = i\nabla_b$, where b is the impact factor for the scattering process, the magnitude of the azimuthal angle correlation depends on the gradient of the parton density.

THE BRIEF REVIEW OF THE MODEL

In this section we briefly review our model, which provides a successful description of the diffractive[11, 12], inclusive cross sections[13] and rapidity correlations[14]. For the description of the angular correlations, it is important to take into account the dependance of the scattering amplitude on the sizes of dipoles, hence in all formulae below, we include this dependance. In our description of the cross sections we previously took $r = 1/m$.

The main ingredient of our model is the BFKL Pomeron Green function, which we determined using the CGC/saturation approach[11, 32]. We calculated this function from the solution of the non-linear Balitsky-Kovchegov equation[19, 21], using the MPSI approximation[59] to sum enhanced diagrams shown in Fig. 1-a. It has the following form:

$$\begin{aligned} G^{\rm dressed}\left(T\right) &= a^2(1-\exp\left(-T\right)) + 2a(1-a)\frac{T}{1+T} + (1-a)^2 G\left(T\right) \\ &\text{with} \quad G\left(T\right) = 1 - \frac{1}{T}\exp\left(\frac{1}{T}\right)\Gamma_0\left(\frac{1}{T}\right) \end{aligned} \tag{2}$$

$$T\left(r_\perp, s, b\right) \;=\; \phi_0\left(r_\perp^2 Q_s^2\left(Y, b\right)\right)^{\bar{\gamma}} \tag{3}$$

where the saturation momentum Q_s is given by

$$Q_s^2\left(b, Y\right) \;=\; Q_{0s}^2\left(b, Y_0\right)\, e^{\lambda\left(Y - Y_0\right)} \tag{4}$$

with

$$Q_{0s}^2\left(b, Y_0\right) \;=\; \left(m^2\right)^{1-1/\bar{\gamma}}\left(S\left(b, m\right)\right)^{1/\bar{\gamma}} \qquad S\left(b, m\right) \;=\; \frac{m^2}{2\pi}e^{-mb} \quad \text{and} \quad \bar{\gamma} \;=\; 0.63 \tag{5}$$

$T\left(r_\perp, s, b\right)$ denotes the dipole - proton amplitude in the vicinity of the saturation scale [60].

In these formulae we take $a = 0.65$, this value was chosen, to reproduce the analytical form for the solution of the BK equation. Parameters λ and ϕ_0, can be estimated in the leading order of QCD, but due to large next-to-leading order corrections, we treat them as parameters of the fit. m is a non-perturbative parameter, which characterizes the large impact parameter behavior of the saturation momentum, as well as the typical size of dipoles that take part in the interactions. The value of $m = 5.25\,GeV$ in our model, justifies our main assumption, that BFKL Pomeron

calculus based on a perturbative QCD approach, is able to describe soft physics, since $m \gg \mu_{soft}$, where μ_{soft} denotes the natural scale for soft processes ($\mu_{soft} \sim \Lambda_{QCD}$ and/or pion mass).

Unfortunately, since the confinement problem is far from being solved, we assume a phenomenological approach for the structure of the colliding hadrons. We use a two channel model, which allows us to calculate the diffractive production in the region of small masses. In this model, we replace the rich structure of the diffractively produced states, by a single state with the wave function ψ_D, a la Good-Walker[61]. The observed physical hadronic and diffractive states are written in the form

$$\psi_h \,=\, \alpha\,\Psi_1 + \beta\,\Psi_2\,; \qquad \psi_D \,=\, -\beta\,\Psi_1 + \alpha\,\Psi_2; \qquad \text{where} \qquad \alpha^2+\beta^2 \,=\, 1; \tag{6}$$

Functions ψ_1 and ψ_2 form a complete set of orthogonal functions $\{\psi_i\}$ which diagonalize the interaction matrix $\mathbf{T}$

$$A^{i'k'}_{i,k} =< \psi_i\,\psi_k|\mathbf{T}|\psi_{i'}\,\psi_{k'} >= A_{i,k}\,\delta_{i,i'}\,\delta_{k,k'}. \tag{7}$$

The unitarity constraints take the form

$$2\,\mathrm{Im}\,A_{i,k}\,(s,b) = |A_{i,k}\,(s,b)\,|^2 + G^{in}_{i,k}(s,b), \tag{8}$$

where $G^{in}_{i,k}$ denotes the contribution of all non diffractive inelastic processes, i.e. it is the summed probability for these final states to be produced in the scattering of a state i off a state k. In Eq. (8) $\sqrt{s} = W$ denotes the energy of the colliding hadrons, and b the impact parameter. A simple solution to Eq. (8) at high energies, has the eikonal form with an arbitrary opacity Ω_{ik}, where the real part of the amplitude is much smaller than the imaginary part.

$$A_{i,k}(s,b) = i\,(1-\exp\,(-\Omega_{i,k}(s,b)))\,, \tag{9}$$

$$G^{in}_{i,k}(s,b) = 1-\exp\,(-2\,\Omega_{i,k}(s,b))\,. \tag{10}$$

Eq. (10) implies that $P^S_{i,k} = \exp\,(-2\,\Omega_{i,k}(s,b))$, is the probability that the initial projectiles (i,k) reach the final state interaction unchanged, regardless of the initial state re-scatterings.

Note, that there is no factor 1/2, its absence stems from our definition of the dressed Pomeron.

model	λ	$\phi_0\ (GeV^{-2})$	$g_1\ (GeV^{-1})$	$g_2\ (GeV^{-1})$	$m(GeV)$	$m_1(GeV)$	$m_2(GeV)$	β	$a_{I\!P I\!P}$
2 channel	0.38	0.0019	110.2	11.2	5.25	0.92	1.9	0.58	0.21

TABLE I: Fitted parameters of the model. The values are taken from Ref.[12].

In the eikonal approximation we replace $\Omega_{i,k}(r_\perp,s,b)$ by

$$\Omega_{i,k}(r_\perp,Y-Y_0,b) \;=\; \int d^2b'\,d^2b''\,g_i\left(\boldsymbol{b}'\right)\,G^{\rm dressed}\left(T\left(r_\perp,Y-Y_0,\boldsymbol{b}''\right)\right)\,g_k\left(\boldsymbol{b}-\boldsymbol{b}'\,-\boldsymbol{b}''\right) \tag{11}$$

We propose a more general approach, which takes into account new small parameters, that come from the fit to the experimental data (see Table 1 and Fig. 1):

$$G_{3I\!P}\Big/ g_i(b=0) \,\ll\, 1; \qquad m \,\gg\, m_1 \text{ and } m_2 \tag{12}$$

The second equation in Eq. (12) leads to the fact that b'' in Eq. (11) is much smaller than b and b', therefore, Eq. (11) can be re-written in a simpler form

$$\begin{aligned}\Omega_{i,k}(r_\perp,Y-Y_0,b) \;&=\; \left(\int d^2b''\,G^{\rm dressed}\left(T\left(r_\perp,Y-Y_0,\boldsymbol{b}''\right)\right)\right)\int d^2b' g_i\left(\boldsymbol{b}'\right)\,g_k\left(\boldsymbol{b}-\boldsymbol{b}'\right)\\ &=\; \tilde{G}^{\rm dressed}\left(r_\perp,Y-Y_0\right)\,\int d^2b' g_i\left(\boldsymbol{b}'\right)\,g_k\left(\boldsymbol{b}-\boldsymbol{b}'\right)\end{aligned} \tag{13}$$

Selecting the diagrams using the first equation in Eq. (12), indicates that the main contribution stems from the net diagrams shown in Fig. 1-b. The sum of these diagrams[12] leads to the following expression for $\Omega_{i,k}(s,b)$

$$\Omega\left(r_\perp,Y-Y_0;b\right) \;=\; \int d^2b'\;\frac{g_i\left(\boldsymbol{b}'\right)\,g_k\left(\boldsymbol{b}-\boldsymbol{b}'\right)\,\tilde{G}^{\rm dressed}\left(r_\perp,Y-Y_0\right)}{1\,+\,G_{3I\!P}\,\tilde{G}^{\rm dressed}\left(r_\perp,Y-Y_0\right)\left[g_i\left(\boldsymbol{b}'\right)+g_k\left(\boldsymbol{b}-\boldsymbol{b}'\right)\right]}; \tag{14}$$

$$g_i\left(b\right) \;=\; g_i\,S_p\left(b;m_i\right); \tag{15}$$

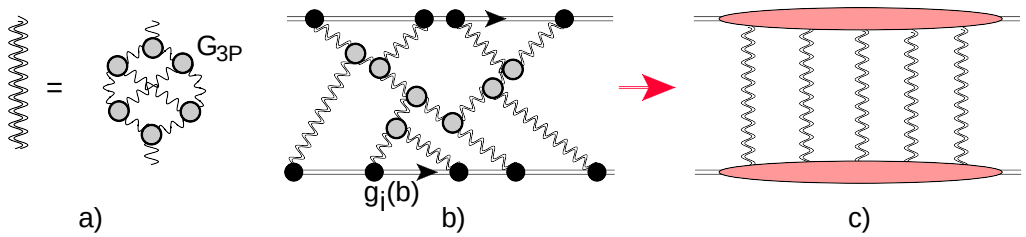

FIG. 1: Fig. 1-a shows the set of the diagrams in the BFKL Pomeron calculus that produce the resulting (dressed) Green function of the Pomeron in the framework of high energy QCD. In Fig. 1-b the net diagrams which include the interaction of the BFKL Pomerons with colliding hadrons are shown. The sum of the diagrams reduces to Fig. 1-c after integration over positions of $G_{3I\!P}$ in rapidity.

where

$$S_p\left(b, m_i\right) \;=\; \frac{1}{4\pi} m_i^3\, b\, K_1\left(m_i b\right) \tag{16}$$

$$\tilde{G}^{\rm dressed}\left(r_\perp, Y - Y_0\right) \;=\; \int d^2b\; G^{\rm dressed}\left(T\left(r_\perp, Y - Y_0, b\right)\right)$$

where $T\left(r_\perp, Y - Y_0, b\right)$ is given by Eq. (3).

Note that $\bar{G}^{\rm dressed}\left(\bar{T}\right)$ does not depend on b. In all previous formulae, the value of the triple BFKL Pomeron vertex is known: $G_{3I\!P} = 1.29\, GeV^{-1}$.

To simplify further discussion, we introduce the notation

$$N^{BK}\left(G^i_{I\!P}\left(r_\perp, Y, b\right)\right) \;=\; a\,\left(1 - \exp\left(-G^i_{I\!P}\left(r_\perp, Y, b\right)\right)\right) \;+\; (1-a)\,\frac{G^i_{I\!P}\left(r_\perp, Y, b\right)}{1 \,+\, G^i_{I\!P}\left(r_\perp, Y, b\right)}, \tag{17}$$

with $a \;=\; 0.65$. Eq. (17) is an analytical approximation to the numerical solution for the BK equation[32]. $G_{I\!P}\left(r_\perp, Y; b\right) \;=\; g_i\left(b\right)\,\tilde{G}^{\rm dressed}\left(r_\perp, Y - Y_0\right)$. We recall that the BK equation sums the 'fan' diagrams.

For the elastic amplitude we have

$$a_{el}(b) \;=\; \left(\alpha^4 A_{1,1} \;+\; 2\alpha^2\,\beta^2\, A_{1,2} \;+\; \beta^4 A_{2,2}\right). \tag{18}$$

CORRELATIONS BETWEEN TWO PARTON SHOWERS

In our previous paper [14], we discovered that in the framework of our model that has been described above, the main source of the long range rapidity correlation, is the correlation between two parton showers. The appropriate Mueller diagrams are shown in Fig. 2. Examining this diagram, we see that the contribution to the double inclusive cross section, differs from the product of two single inclusive cross sections. This difference generates the rapidity correlation function, which is defined as

$$R\left(y_1, y_2\right) \;=\; \frac{\frac{1}{\sigma_{in}}\frac{d^2\sigma}{dy_1\, dy_2}}{\frac{1}{\sigma_{in}}\frac{d\sigma}{dy_1}\,\frac{1}{\sigma_{in}}\frac{d\sigma}{dy_2}} \;-\; 1 \tag{19}$$

There are two reasons for the difference between the double inclusive cross section due to production of two parton showers, and the products of inclusive cross sections: the first, is that in the expression for the double inclusive cross section, we integrate the product of the single inclusive inclusive cross sections, over b. The second, is that the summation over i and k for the product of single inclusive cross sections, is for fixed i and k.

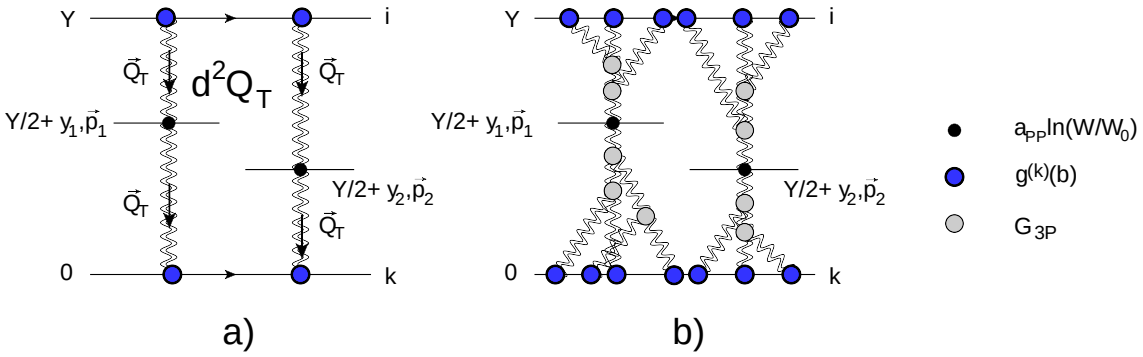

FIG. 2: The Mueller diagram for the rapidity correlation between two particles produced in two parton showers. Fig. 2-a shows the first Mueller diagram, whileFig. 2-b indicates the structure of general diagrams. The double wavy lines describe the dressed BFKL Pomerons. The blobs stand for the vertices as shown in the legend.

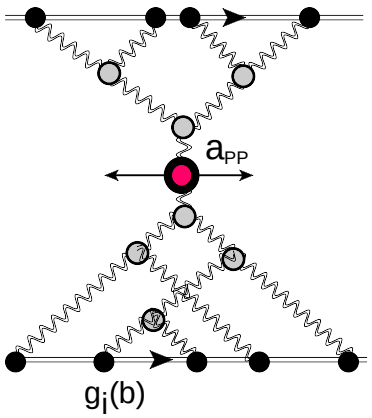

FIG. 3: The Mueller diagram for the single inclusive cross section. The double wavy lines describe the resulting Green function of the BFKL Pomerons ($\tilde{G}^{\rm dressed}$). The blobs stand for the vertices which are the same as in Fig. 2.

Introducing the following new function, enables us to write the analytical expression for the double inclusive cross section:

$$
\begin{aligned}
I^{(i,k}\left(y,b\right) \;&=\; a_{I\!P I\!P}\,\ln\left(W/W_0\right) \\
&\times \int d^2b'\; N^{BK}\left(g^{(i)}\,S\left(m_i,b'\right)\tilde{G}^{\rm dressed}\left(r_\perp=1/m,\frac{1}{2}Y+y\right)\right) \\
&N^{BK}\left(g^{(k)}\,S\left(m_k,\boldsymbol{b}-\boldsymbol{b}^{'}\right)\tilde{G}^{\rm dressed}\left(r_\perp=1/m,\frac{1}{2}Y-y\right)\right)
\end{aligned}
\tag{20}
$$

Using Eq. (20) we can write the double inclusive cross section in the form

$$
\begin{aligned}
\frac{d^2\sigma^{2\text{ parton showers}}}{dy_1\;dy_2} \;&=\; \int d^2p_{1T}\,d^2p_{2T}\frac{d^2\sigma^{2\text{ parton showers}}}{dy_1\;dy_2\,d^2p_{1T}\,d^2p_{2T}} \;=\; \int d^2b\,\Big\{\alpha^4\,I^{(1,1)}\left(y_1,b\right)\,I^{(1,1)}\left(y_2,b\right) \\
&\alpha^2\,\beta^2\,\Big(I^{(1,2)}\left(y_1,b\right)\,I^{(1,2)}\left(y_2,b\right)\;+\;I^{(2,1)}\left(y_1,b\right)\,I^{(2,1)}\left(y_2,b\right)\Big)\;+\;\beta^4\,I^{(2,2)}\left(y_1,b\right)\,I^{(2,2)}\left(y_2,b\right)\Big\}
\end{aligned}
\tag{21}
$$

Comparing Eq. (21) with the square of the single inclusive cross section (see below Eq. (23)) , we note the different powers of α and β, which reflect the different summation over i and k, as well as different integration over b.

Other sources can contribute to the correlation function $R\,(y_1, y_2)$ which is defined as

$$R\,(y_1,y_2) \;=\; \sigma_{NSD}\left\{\frac{d^2\sigma^{2\text{ parton showers}}}{dy_1\;dy_2} \;+\; \frac{d^2\sigma^{1\text{ parton shower}}_{\text{semi-enhanced}}}{dy_1\;dy_2} \;+\; \frac{d^2\sigma^{1\text{ parton shower}}_{\text{enhanced}}}{dy_1\;dy_2}\right\}\Bigg/\left\{\frac{d\sigma}{dy_1}\,\frac{d\sigma}{dy_2}\right\} \;-\; 1 \tag{22}$$

In Ref.[14] we showed that both semi-enhanced and enhanced diagrams which are related to the correlations in one patron shower, give negligible contributions, and can be neglected.

We have discussed in Ref.[14] the rapidity correlations that are generated by Eq. (21). In the present paper we wish to consider the correlations in the azimuthal angle between two momenta of produced gluons: $\boldsymbol{p}_{1,\perp}$ and $\boldsymbol{p}_{2,\perp}$.

The single inclusive cross section can be calculate using the following formula[13]

$$\begin{aligned}\frac{d\sigma}{dy} \;&=\; \int d^2p_T\,\frac{d\sigma}{dy\,d^2p_T} \;=\; a_{I\!P I\!P}\,\ln\left(W/W_0\right)\Bigg\{\alpha^4\,In^{(1)}\left(\frac{1}{2}Y+y\right)\,In^{(1)}\left(\frac{1}{2}Y-y\right)\\ &+\;\alpha^2\beta^2\Big(In^{(1)}\left(\frac{1}{2}Y+y\right)\,In^{(2)}\left(\frac{1}{2}Y-y\right)\,+\,In^{(2)}\left(\frac{1}{2}Y+y\right)\,In^{(1)}\left(\frac{1}{2}Y-y\right)\Big)\\ &+\;\beta^4\,In^{(2)}\left(\frac{1}{2}Y+y\right)\,In^{(2)}\left(\frac{1}{2}Y-y\right)\Bigg\}\end{aligned} \tag{23}$$

where Y denotes the total rapidity of the colliding particles, and y is the rapidity of produced hadron. $In^{(i)}(y)$ is given by

$$In^{(i)}\,(y) \;=\; \int d^2b\;N^{BK}\left(g^{(i)}\,S\,(m_i,b)\;\tilde{G}_{I\!P}\,(r_\perp = 1/m, Y-Y_0)\right) \tag{24}$$

and $a_{I\!P I\!P}$ is a fitted parameter, that was determined in Ref.[13] (see Table 1).

CALCULATION OF THE FIRST DIAGRAM

In this section we calculate the first Mueller diagram shown in Fig. 2-a. We reproduce in an alternative way, the main results of Ref. [36]. We start from the calculation of the inclusive production, from one BFKL Pomeron, which enters this diagram at fixed momentum transfer $\boldsymbol{Q}_T$. Note, that the inclusive cross section, shown in Fig. 3, is determined by the same BFKL Pomeron, but at $Q_T = 0$.

Inclusive production from one BFKL Pomeron

The BFKL Pomeron: generalities

The general solution to the BFKL equation for the scattering amplitude of two dipoles with the sizes r_1 and r_2, has been derived in Ref.[24], and has the form

$$\begin{aligned}&N_{I\!P}\,(r_1,r_2;Y,b) \;=\\ &\sum_{n=0}^{\infty}\int\frac{d\gamma}{2\,\pi\,i}\,\phi^{(n)}_{in}(\gamma;r_2)\;d^2\,R_1\;d^2\,R_2\,\delta(\boldsymbol{R}_1-\boldsymbol{R}_2-\boldsymbol{b})\,e^{\omega(\gamma,n)\,Y}\,E^{\gamma,n}\,(r_1,R_1)\;E^{1-\gamma,n}\,(r_2,R_2)\end{aligned} \tag{25}$$

with

$$\omega(\gamma,n) \;=\; \bar{\alpha}_S\chi(\gamma,n) \;=\; \bar{\alpha}_S\,(2\psi\,(1) \;-\; \psi\,(\gamma+|n|/2) \;-\; \psi\,(1-\gamma+|n|/2))\,; \tag{26}$$

where $\psi\,(\gamma) \;=\; d\ln\Gamma\,(\gamma)\,/d\gamma$ and $\Gamma\,(\gamma)$ is Euler gamma function. Functions $E^{n,\gamma}\,(\rho_{1a},\rho_{2a})$ are given by the following equations.

$$E^{n,\gamma}\,(\rho_{1a},\rho_{2a}) \;=\; \left(\frac{\rho_{12}}{\rho_{1a}\,\rho_{2a}}\right)^{1-\gamma+n/2}\left(\frac{\rho^*_{12}}{\rho^*_{1a}\,\rho^*_{2a}}\right)^{1-\gamma-n/2}, \tag{27}$$

In Eq. (27) we use complex numbers to characterize the point on the plane

$$\rho_i = x_{i,1} + i\, x_{i,2}; \quad \rho^*_i = x_{i,1} - i\, x_{i,2} \tag{28}$$

where the indices 1 and 2 denote two transverse axes. Notice that

$$\rho_{12}\,\rho^*_{12} \;=\; r_i^2; \qquad \rho_{1a}\,\rho^*_{1a} \;=\; \left(\boldsymbol{R}_i \;-\; \frac{1}{2}\boldsymbol{r}_i\right)^2 \qquad \rho_{2a}\,\rho^*_{2a} \;=\; \left(\boldsymbol{R}_i \;+\; \frac{1}{2}\boldsymbol{r}_i\right)^2 \tag{29}$$

At large values of Y, the main contribution stems from the first term with $n = 0$. For this term Eq. (27) can be re-written in the form

$$E^{\gamma,0}\left(r_i, R_i\right) \;=\; \left(\frac{r_i^2}{(\boldsymbol{R}_i \;+\; \frac{1}{2}\boldsymbol{r}_i)^2\;(\boldsymbol{R}_i \;-\; \frac{1}{2}\boldsymbol{r}_i)^2}\right)^{1-\gamma}. \tag{30}$$

The integrals over R_1 and R_2 were taken in Refs.[24, 63] and at $n = 0$ we have

$$H^{\gamma}\left(w, w^*\right) \;\equiv\; \int d^2\, R_1\, E^{\gamma,0}\left(r_1, R_1\right)\; E^{1-\gamma,0}\left(r_2, \boldsymbol{R}_1 \;-\; \boldsymbol{b}\right) \;= \tag{31}$$

$$\frac{(\gamma - \frac{1}{2})^2}{(\gamma(1-\gamma))^2}\Big\{b_\gamma\, w^\gamma\, w^{*\gamma}\, F\left(\gamma, \gamma, 2\gamma, w\right)\; F\left(\gamma, \gamma, 2\gamma, w^*\right) \;+$$

$$b_{1-\gamma} w^{1-\gamma} w^{*1-\gamma} F\left(1-\gamma, 1-\gamma, 2-2\gamma, w\right)\; F\left(1-\gamma, 1-\gamma, 2-2\gamma, w^*\right)\Big\}$$

where F is hypergeometric function [64]. In Eq. (31) $w\, w^*$ is equal to

$$w\, w^* \;=\; \frac{r_1^2\, r_2^2}{\left(\boldsymbol{b} - \frac{1}{2}\left(\boldsymbol{r}_1 \;-\; \boldsymbol{r}_2\right)\right)^2\;\left(\boldsymbol{b} \;+\; \frac{1}{2}\left(\boldsymbol{r}_1 \;-\; \boldsymbol{r}_2\right)\right)^2} \tag{32}$$

and b_γ is equal to

$$b_\gamma \;=\; \pi^3\, 2^{4(1/2-\gamma)}\, \frac{\Gamma\left(\gamma\right)}{\Gamma\left(1/2-\gamma\right)}\, \frac{\Gamma\left(1-\gamma\right)}{\Gamma\left(1/2+\gamma\right)}. \tag{33}$$

Finally, the solution at large Y has the form

$$N_{I\!P}\left(r_1, r_2; Y, b\right) \;=\; \int \frac{d\gamma}{2\,\pi\, i}\, e^{\omega(\gamma,0)\, Y}\, H^{\gamma}\left(w, w^*\right) \tag{34}$$

In the vicinity of the saturation scale $N_{I\!P}$ takes the form (see Refs. [60, 65])

$$N_{I\!P}\left(r_1, r_2; Y, b\right) \;=\; \frac{\left(\gamma_{cr} - \frac{1}{2}\right)^2}{\gamma_{cr}(1-\gamma_{cr})}\, b_{\gamma_{cr}}\Big(w w^* e^{\kappa Y})^{1-\gamma_{cr}}$$

$$= \;\frac{\left(\gamma_{cr} - \frac{1}{2}\right)^2}{\gamma_{cr}(1-\gamma_{cr})}\, b_{\gamma_{cr}}\left(\left(\frac{r_1^2\, r_2^2}{\left(\boldsymbol{b} - \frac{1}{2}\left(\boldsymbol{r}_1 \;-\; \boldsymbol{r}_2\right)\right)^2\;\left(\boldsymbol{b} \;+\; \frac{1}{2}\left(\boldsymbol{r}_1 \;-\; \boldsymbol{r}_2\right)\right)^2}\right) e^{\bar{\alpha}_S \frac{\chi(\gamma_{cr})}{1-\gamma_{cr}}\, Y}\right)^{1-\gamma_{cr}} \tag{35}$$

$$\xrightarrow{r_2 \gg r_1} \quad \phi_0\left(r_1^2 Q_s^2\left(r_2, b; Y\right)\right)^{1-\gamma_{cr}} \quad \text{with} \quad Q_s^2\left(r_2, b; Y\right) \;= \frac{r_2^2\, e^{\bar{\alpha}_S \frac{\chi(\gamma_{cr})}{1-\gamma_{cr}}\, Y}}{\left(\boldsymbol{b} - \frac{1}{2}\boldsymbol{r}_2\right)^2\;\left(\boldsymbol{b} \;+\; \frac{1}{2}\boldsymbol{r}_2\right)^2} \tag{36}$$

where (see Refs.[16, 60, 62])

$$\frac{\chi\left(\gamma_{cr}\right)}{1-\gamma_{cr}} \;=\; -\frac{d\chi\left(\gamma_{cr}\right)}{d\gamma_{cr}} \quad \text{where} \quad \chi\left(\gamma\right) \;=\; 2\psi\left(1\right) \;-\; \psi\left(\gamma\right) \;-\; \psi\left(1-\gamma\right) \leftarrow \text{kernel of the BFKL equation} \tag{37}$$

Below we denote by $\bar{\gamma} = 1 - \gamma_{cr}$, and will use Eq. (35) and Eq. (36) in the momentum transfer representation, viz.

$$N_{I\!P}\left(r_1, r_2; Y, Q_T\right) \;=\; \int d^2 b\; e^{i\boldsymbol{Q}_T \cdot \boldsymbol{b}}\;\; N_{I\!P}\left(r_1, r_2; Y, b\right) \tag{38}$$

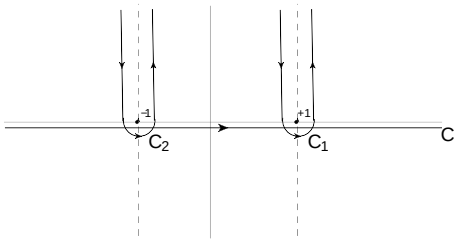

FIG. 4: Contours of integration in Eq. (40).

The integral of Eq. (38) with $N_{I\!P}\left(r_1,r_2;Y,b\right)$ from Eq. (35) can be evaluated using the complex number description for the point on the plane, (see Eq. (28) and Eq. (29)). The integral has the form[24, 63]

$$N_{I\!P}\left(r_1,r_2;Y,Q_T\right) = \left(r_1^2\,r_2^2\right)^{\bar\gamma}\; e^{\bar\alpha_S\,\chi(\gamma_{cr})\,Y}\int d\rho_b\; e^{i\rho_Q^*\rho_b}\left(\frac{1}{\rho_b^2-\rho_{12}^2}\right)^{\gamma}\int d\rho_b^*\; e^{i\rho_Q\rho_b^*}\left(\frac{1}{\rho_b^{*2}-\rho_{12}^{*2}}\right)^{\gamma} \tag{39}$$

Using new variables $t=\rho_b/\rho_{12}$ and $t^*=\rho_b^*/\rho_{12}$ and the integral representation of Hankel functions (see formulae **8.422(1,2)** in Ref. [64])

$$H_\nu^{(1,2)}\left(z\right) \;=\; \frac{\Gamma\left(\frac12-\nu\right)}{\pi i\Gamma\left(\frac12\right)}\left(\frac12 z\right)^{\nu}\oint_{C_{1,2}} dt e^{izt}\left(t^2-1\right)^{\nu-\frac12} \tag{40}$$

where contours C_1 and C_2 are shown in Fig. 4, we obtain

$$N_{I\!P}\left(r_1,r_2;Y,Q_T\right) \;=\; C^2(\gamma)\,r_{12}^2\,e^{\bar\alpha_S\,\chi(\gamma)\,Y}\;\left(\frac{r_1^2r_2^2}{r_{12}^4}\right)^{\gamma}\;\left(Q^2r_{12}^2\right)^{-\frac12+\gamma}\;\;J_{\frac12-\gamma}\left(\rho_Q^*\rho_{12}\right)J_{\frac12-\gamma}\left(\rho_Q\rho_{12}^*\right) \tag{41}$$

where $2J_\nu(z)=H^{(1)}\left(z\right)+H_\nu^{(2)}\left(z\right)$; $\boldsymbol{r}_{12}=\frac12\left(\boldsymbol{r}_1-\boldsymbol{r}_2\right)$ and

$$C(\gamma) \;=\; 2^{-\frac52+\gamma}\pi\frac{\Gamma\left(\frac12\right)}{\Gamma\left(\gamma\right)} \tag{42}$$

Two limits will be useful for further presentation:

$$N_{I\!P}\left(r_1,r_2;Y,Q_T\right) \quad\xrightarrow{Q_T\to0}\quad C^2(\gamma)\,r_{12}^2\,e^{\bar\alpha_S\,\chi(\gamma)\,Y}\;\left(\frac{r_1^2r_2^2}{r_{12}^4}\right)^{\gamma} \tag{43}$$

$$\xrightarrow{Q_T^2\,r_{12}^2\gg1}\quad \frac{2}{\pi}\,C^2(\gamma)\,r_{12}^2\,e^{\bar\alpha_S\,\chi(\gamma)\,Y}\;\left(\frac{r_1^2r_2^2}{r_{12}^4}\right)^{\gamma}\;\left(Q^2r_{12}^2\right)^{-1+\gamma}\cos^2\left(\pi\gamma/2\right)e^{i\boldsymbol{Q}\cdot\boldsymbol{r}_{12}} \tag{44}$$

Eq. (43) can be re-written at $r_1\ll r_2$ in the form :

$$N_{I\!P}\left(r_1,r_2;Y,Q_T\right) \quad\xrightarrow{Q_T\to0,r_1\ll r_2}\quad C^2(\gamma)\,r_{12}^2\left(r_1^2Q_s^2\left(Y,r_2\right)\right)^{\gamma} \quad\text{with}\;\; Q_s^2 \;=\; \frac{1}{r_2^2}\,e^{\bar\alpha_S\,\frac{\chi(\gamma)}{\gamma}\,Y};$$

$$\xrightarrow{Q_Tr_2\gg1,r_1\ll r_2}\quad \frac{2}{\pi}\,C^2(\gamma)\,\cos^2\left(\pi\gamma/2\right)e^{i\boldsymbol{Q}\cdot\boldsymbol{r}_{12}}\,e^{\bar\alpha_S\,\chi(\gamma)\,Y}\frac{1}{Q_T^2}\left(Q_T^2\,r_1^2\right)^{\gamma} \tag{45}$$

General formula

In this subsection we calculate the cross section for the inclusive production of a gluon jet with transverse momentum $p_\perp$ at rapidity Y_1, in the collision of two dipoles with sizes r_1 and r_2, at rapidity Y, and at impact parameter b. The general formula which shows k_T-factorization [66], has been derived in Ref.[67] and has the form

$$\frac{d\sigma}{d^2b\,dY_1\,d^2p_\perp} \;= \tag{46}$$

$$\frac{2C_F}{\alpha_s(2\pi)^4}\,\frac{1}{p_\perp^2}\int d^2\boldsymbol{B}\,d^2\boldsymbol{r}_\perp\,e^{i\boldsymbol{p}_\perp\cdot\boldsymbol{r}_\perp}\;\nabla_\perp^2\,N^G\left(\frac12Y-y_1;r_\perp,r_1;b\right)\;\nabla_\perp^2\,N^G\left(\frac12Y+y_1;r_\perp,r_2;|\boldsymbol{b}-\boldsymbol{B}|\right)$$

where

$$N^G\left(Y;r_\perp,r_i;b\right)\;=\;2\,N\left(Y;r_\perp,r_i;b\right)\;-\;N^2\left(Y;r_\perp,r_i;b\right), \tag{47}$$

For one Pomeron exchange Eq. (47) reduces to the following equation

$$N^G_{I\!P}\left(Y;r_\perp,r_i;b\right)\;=\;2\,N_{I\!P}\left(Y;r_\perp,r_i;b\right) \tag{48}$$

Plugging Eq. (48) into Eq. (46) we have

$$\begin{aligned}&N^{\rm incl}_{I\!P}\left(Y,r_1,r_2,b,p_\perp,Y_1\right)=\\&\frac{8\,C_F}{\alpha_s(2\pi)^4}\,\frac{1}{p_\perp^2}\int d^2\boldsymbol{B}\,d^2\boldsymbol{r}_\perp\,e^{i\boldsymbol{p}_\perp\cdot\boldsymbol{r}_\perp}\;\nabla^2_\perp\,N_{I\!P}\left(Y_1;r_\perp,r_1;B\right)\;\nabla^2_\perp\,N_{I\!P}\left(Y-Y_1;r_\perp,r_2;|\boldsymbol{b}-\boldsymbol{B}|\right)\end{aligned} \tag{49}$$

Note, that b is the difference of the impact parameters between scattering dipoles, while B is the impact parameter of the produced gluon with respect to the dipole of size r_1.

It is more convenient to use $\nabla^2_\perp\,N_{I\!P}\left(Y_1;r_\perp,r_1;b\right)$ in momentum representation, namely,

$$\int d^2b\,e^{i\boldsymbol{Q}_T\cdot\boldsymbol{b}}\;\nabla^2_\perp\,N_{I\!P}\left(Y_1;r_\perp,r_1;b\right)\;=\;\nabla^2_\perp\,N_{I\!P}\left(Y_1;r_\perp,r_1;Q_T\right) \tag{50}$$

Using Eq. (41) for $N_{I\!P}\left(Y_1;r_\perp,r_1;Q_T\right)$ and $\nabla^2_r\;=\;4\,\partial_\rho\partial_{\rho^*}$ we obtain(denoting $r_\perp\equiv r_0$)

$$\begin{aligned}\nabla^2_\perp\,N_{I\!P}\left(Y_1;r_\perp,r_1;Q_T\right)\;&=\;\int_{\epsilon-i\infty}^{\epsilon+i\infty}\frac{d\gamma}{2\pi i}\;4\;C^2(\gamma)\,r_{01}^2\,e^{\bar\alpha_S\,\chi(\gamma)\,Y}\;\left(\frac{r_1^2r_0^2}{r_{01}^4}\right)^\gamma\;\left(Q^2r_{01}^2\right)^{-\frac{1}{2}+\gamma}\\&\times\;\left\{\left(\frac{\gamma}{\rho_r}-\frac{\frac{1}{2}+\gamma}{\rho_{01}}\right)J_{\frac{1}{2}-\gamma}\left(\rho^*_Q\rho_{01}\right)+\frac{1}{2}\rho^*_Q\left(J_{-\frac{1}{2}-\gamma}\left(\rho^*_Q\rho_{01}\right)\;-\;J_{-\frac{3}{2}-\gamma}\left(\rho^*_Q\rho_{01}\right)\right)\right\}\\&\times\;\left\{\left(\frac{\gamma}{\rho^*_r}-\frac{\frac{1}{2}+\gamma}{\rho^*_{01}}\right)J_{\frac{1}{2}-\gamma}\left(\rho_Q\rho^*_{01}\right)+\frac{1}{2}\rho_Q\left(J_{-\frac{1}{2}-\gamma}\left(\rho_Q\rho^*_{01}\right)\;-\;J_{-\frac{3}{2}-\gamma}\left(\rho_Q\rho^*_{01}\right)\right)\right\}\end{aligned} \tag{51}$$

We need to estimate

$$N^{\rm incl}_{I\!P}\left(Y,r_1,r_2,Q_T,p_\perp,Y_1\right)\;=\;\int d^2b\;e^{i\boldsymbol{Q}_T\cdot\boldsymbol{b}}\,N^{\rm incl}_{I\!P}\left(Y,r_1,r_2,b,p_\perp,Y_1\right) \tag{52}$$

for calculating the diagrams of Fig. 2-a. From Eq. (49) and Eq. (51) we obtain

$$\begin{aligned}&N^{\rm incl}_{I\!P}\left(Y,y_1,r_1,r_2,Q_T,p_\perp,Y_1\right)\;=\\&\frac{8\,C_F}{\alpha_s(2\pi)^4}\,\frac{1}{p_\perp^2}\int d^2\boldsymbol{r}_\perp\,e^{i\boldsymbol{p}_\perp\cdot\boldsymbol{r}_\perp}\;\nabla^2_\perp\,N_{I\!P}\left(y_1;r_\perp,r_1;Q_T\right)\;\nabla^2_\perp\,N_{I\!P}\left(Y-y_1;r_\perp,r_2;Q_T\right)\end{aligned} \tag{53}$$

Note, the dependence on y_1 is very weak since $N_{I\!P}\left(y_1;r_\perp,r_1;Q_T\right)\;\propto\exp\left(\bar\alpha_S\chi(\gamma)\,y_1\right)$.

Azimuthal angle dependance

As we have discussed in the introduction, the azimuthal angle correlation arises from the terms $\left(\boldsymbol{p}_{\perp,1}\cdot\boldsymbol{Q}_T\right)^2$ and $\left(\boldsymbol{p}_{\perp,2}\cdot\boldsymbol{Q}_T\right)^2$, after integration over Q_T in the Pomeron loop in the diagram of Fig. 2-a, since $\int d^2Q_T\left(\boldsymbol{p}_{\perp,1}\cdot\boldsymbol{Q}_T\right)^2\left(\boldsymbol{p}_{\perp,2}\cdot\boldsymbol{Q}_T\right)^2\;\to\;\left(\boldsymbol{p}_{\perp,1}\cdot\boldsymbol{p}_{\perp,2}\right)^2$. Such terms in the coordinate representation that we are using here, stem from the terms $\left(\boldsymbol{r}_{12}\cdot\boldsymbol{Q}_T\right)^2$ and $\left(\boldsymbol{r}^{'}_{12}\cdot\boldsymbol{Q}_T\right)^2$ in $N_{I\!P}\left(r_1,r_2,Y,Q_T\right)$ and $N_{I\!P}\left(r^\prime_1,r^\prime_2,Y,Q_T\right)$ (see Eq. (41)). These terms come from $J_{\frac{1}{2}-\gamma}\left(\rho^*_Q\,\rho_{12}\right)\;J_{\frac{1}{2}-\gamma}\left(\rho_Q\,\rho^*_{12}\right)$. For small Q_T we can see how these terms appear by expanding $J_{\frac{1}{2}-\gamma}$.

Indeed,

$$\begin{aligned}&\left(Q^2r_{12}^2\right)^{-\frac{1}{2}+\gamma}\;J_{\frac{1}{2}-\gamma}\left(\rho^*_Q\,\rho_{12}\right)\;J_{\frac{1}{2}-\gamma}\left(\rho_Q\,\rho^*_{12}\right)=\\&=\;\left(\frac{1}{2^{\frac{1}{2}-\gamma}\,\Gamma\left(\frac{3}{2}-\gamma\right)}\right)^2\left\{1+\frac{1}{2(-3+2\,\gamma)}Q_T^2r_{12}^2e^{2i(\phi-\psi)}\right\}\left\{1+\frac{1}{2(-3+2\,\gamma)}Q_T^2r_{12}^2e^{-2i(\phi-\psi)}\right\}\\&\to\;\left(\frac{1}{2^{\frac{1}{2}-\gamma}\,\Gamma\left(\frac{3}{2}-\gamma\right)}\right)^2\left\{1+\frac{1}{(-3+2\,\gamma)}Q_T^2r_{12}^2\cos\left(2(\phi-\psi)\right)+\left(\frac{1}{2(-3+2\,\gamma)}\right)^2Q_T^4r_{12}^4\right\}\end{aligned} \tag{54}$$

$$\to \left(\frac{1}{2^{\frac{1}{2}-\gamma}\,\Gamma\left(\frac{3}{2}-\gamma\right)}\right)^2 \left\{1+\frac{1}{(-3+2\bar{\gamma})}\left(2\left(\boldsymbol{Q}_T\cdot\boldsymbol{r}_{12}\right)^2-Q_T^2 r_{12}^2\right)+\left(\frac{1}{2(-3+2\,\gamma)}\right)^2 Q_T^4 r_{12}^4\right\}$$

In Eq. (54) we use the representation of complex numbers in the polar coordinates, for example, $\rho_Q = Qe^{i\phi}$ and $\rho_Q^* = Qe^{-i\phi}$. The same type of contributions come from Eq. (51).

For $Q_T r_{12} \gg 1$ we have the same features since

$$\begin{aligned}
&N_{I\!P}\left(r_1,r_2;Y,Q_T\right) \xrightarrow{Q_T^2\, r_{12}^2 \gg 1} \\
&,\int_{\epsilon-i\infty}^{\epsilon+i\infty}\frac{d\gamma}{2\pi i}\;C^2(\gamma)\,\frac{2}{\pi}\,r_{12}^2\,e^{\bar{\alpha}_S\,\chi(\gamma_{cr})\,Y}\,\left(\frac{r_1^2 r_2^2}{r_{12}^4}\right)^{\gamma}\,\left(Q_T^2 r_{12}^2\right)^{-1+\gamma}\cos^2\left(\pi\gamma/2\right)e^{i\boldsymbol{Q}_T\cdot\boldsymbol{r}_{12}} \\
&\left\{(1/8)(\gamma\,(\gamma-2)(1-\gamma^2))+Q_T^2 r_{12}^2\,e^{i2(\phi-\psi)}\right\}\left\{(1/8)(\bar{\gamma}\,(\gamma-2)(1-\gamma^2))+Q_T^2 r_{12}^2\,e^{-i2(\phi-\psi)}\right\}\Big/Q_T^4 r_{12}^4 \\
&=\int_{\epsilon-i\infty}^{\epsilon+i\infty}\frac{d\gamma}{2\pi i}\;C^2(\gamma)\;\frac{2}{\pi}\,r_{12}^2\,e^{\bar{\alpha}_S\,\chi(\gamma_{cr})\,Y}\,\left(\frac{r_1^2 r_2^2}{r_{12}^4}\right)^{\gamma}\,\left(Q_T^2 r_{12}^2\right)^{-3+\gamma}\cos^2\left(\pi\gamma/2\right)e^{i\boldsymbol{Q}_T\cdot\boldsymbol{r}_{12}} \\
&\left\{\left[(1/8)(\gamma\,(\bar{\gamma}-2)(1-\gamma^2))\right]^2+(1/4)(\gamma\,(\gamma-2)(1-\gamma^2))\left(2\left(\boldsymbol{Q}_T\cdot\boldsymbol{r}_{12}\right)^2-Q_T^2 r_{12}^2\right)+Q_T^4 r_{12}^4\right\}
\end{aligned} \tag{55}$$

However, the largest contribution at $r \ll r_1$ and $r \ll r_2$ comes from Eq. (51), which can be re-written as

$$\begin{aligned}
&\nabla_\perp^2\, N_{I\!P}\left(Y_1;r_\perp,r_1;Q_T\right)\;\to \\
&\qquad\int_{\epsilon-i\infty}^{\epsilon+i\infty}\frac{d\gamma}{2\pi i}\;C^2(\gamma)\,r_{01}^2\,e^{\bar{\alpha}_S\,\chi(\gamma)\,Y}\,\left(\frac{r_0^2 r_1^2}{r_{01}^4}\right)^{\gamma}\,\left(Q^2 r_{01}^2\right)^{-\frac{1}{2}+\gamma}\frac{\gamma^2}{r^2}\,J_{\frac{1}{2}-\gamma}\left(\rho_Q^*\rho_{01}\right)\,J_{\frac{1}{2}-\gamma}\left(\rho_Q\rho_{01}^*\right)
\end{aligned} \tag{56}$$

where $r_0 \equiv r_\perp$.

Note, that at $Q_T \to 0$ Eq. (56) reduces to

$$\begin{aligned}
&\nabla_\perp^2\, N_{I\!P}\left(Y_1;r_\perp,r_1;Q_T\right)\;\to \\
&\int_{\epsilon-i\infty}^{\epsilon+i\infty}\frac{d\gamma}{2\pi i}\;4\,C^2(\gamma)\,r_{01}^2\,e^{\bar{\alpha}_S\,\chi(\gamma)\,Y}\,\left(\frac{r_0^2 r_1^2}{r_{01}^4}\right)^{\gamma}\,\left(\frac{2^{-\frac{1}{2}\gamma}}{\Gamma\left(3/2-\gamma\right)}\right)^2\frac{\gamma^2}{r^2}\left\{1-\frac{1}{(3-2\gamma)}\left(\rho_Q^2\rho_{01}^{*2}\;+\;\rho_Q^{*2}\rho_{01}^2\right)\right\} \\
&=\int_{\epsilon-i\infty}^{\epsilon+i\infty}\frac{d\gamma}{2\pi i}\;4\,C^2(\gamma)\,r_{01}^2\,e^{\bar{\alpha}_S\,\chi(\gamma)\,Y}\,\left(\frac{r_0^2 r_1^2}{r_{01}^4}\right)^{\gamma}\,\left(\frac{2^{-\frac{1}{2}\gamma}}{\Gamma\left(3/2-\gamma\right)}\right)^2\frac{\gamma^2}{r^2}\left\{1-\frac{2}{(3-2\gamma)}\,\left(\boldsymbol{Q}_T\boldsymbol{r}_{01}\right)^2\right\} \\
&=\int_{\epsilon-i\infty}^{\epsilon+i\infty}\frac{d\gamma}{2\pi i}\;4\;C^2(\gamma)\,r_{01}^2\,e^{\bar{\alpha}_S\,\chi(\gamma)\,Y}\,\left(\frac{r_0^2 r_1^2}{r_{01}^4}\right)^{\gamma}\,\left(\frac{2^{-\frac{1}{2}\gamma}}{\Gamma\left(3/2-\gamma\right)}\right)^2\frac{\gamma^2}{r^2}\left\{1-\frac{2}{(3-2\,\gamma)}\,\left(\boldsymbol{Q}_T\boldsymbol{r}\right)^2\right\}
\end{aligned} \tag{57}$$

To calculate the production of the gluon with the transverse momentum $p_{1,\perp}$, we need to plug Eq. (57) into Eq. (34) and Eq. (53).

Angular dependence of the double inclusive cross section

The contribution to the double inclusive production from the diagram of Fig. 2 takes the general form

$$\begin{aligned}
&\frac{d^2\sigma^{2\text{ parton showers}}}{dy_1\;dy_2,d^2p_{1,\perp}d^2p_{2,\perp}}\;= \\
&\sum_{i=1,j=1}^{i=2,j=2}\alpha_i^2\,\alpha_j^2\int g_i^2\left(Q_T\right)\,g_j^2\left(Q_T\right)\,N_{I\!P}^{\rm incl}\left(Y,y_1,r_1,r_2,Q_T,p_{1,\perp},Y_1\right)\,N_{I\!P}^{\rm incl}\left(Y,y_2,r_1,r_2,Q_T,p_{2,\perp},Y_1\right)\,\frac{d^2Q_T}{4\pi^2}
\end{aligned} \tag{58}$$

where $\alpha_1=\alpha,\alpha_2=\beta$ and $g_i\left(Q_T\right)\;=\;g_i\int d^2b\,e^{i\boldsymbol{Q}_T\cdot\boldsymbol{b}}\,S_{I\!P}\left(b,m_i\right)\;=\;g_i/(1+Q_T^2/m_i^2)^2$, as it follows from Eq. (16).

Substituting Eq. (57) into Eq. (53) we obtain

$$N^{\rm incl}_{I\!P}\left(Y,y_1,r_1,r_2,Q_T,p_{1\perp},Y_1\right) \;=\; \frac{8\,C_F}{\bar{\alpha}_S(2\pi)^4}\,\frac{1}{p^2_{1\perp}}\int d^2\boldsymbol{r}_0\,e^{i\boldsymbol{p}_{1,\perp}\cdot\boldsymbol{r}_0} \tag{59}$$

$$\int_{\epsilon-i\infty}^{\epsilon+i\infty}\frac{d\gamma_1}{2\pi i}\;4\;C^2(\gamma_1)\,r^2_{01}\,e^{\bar{\alpha}_S\,\chi(\gamma_1)\left(\frac{1}{2}Y-y_1\right)}\,\left(\frac{r^2_0r^2_1}{r^4_{01}}\right)^{\gamma_1}\,\left(\frac{2^{-\frac{1}{2}\gamma_1}}{\Gamma\left(3/2-\gamma_1\right)}\right)^2\frac{\gamma^2_1}{r^2_0}\left\{1-\frac{2}{(3-2\,\gamma_1)}\;(\boldsymbol{Q}_T\boldsymbol{r}_0)^2\right\}$$

$$\int_{\epsilon-i\infty}^{\epsilon+i\infty}\frac{d\gamma_2}{2\pi i}\;4\;C^2(\gamma_2)\,r^2_{01}\,e^{\bar{\alpha}_S\,\chi(\gamma_2)\left(\frac{1}{2}Y+y_1\right)}\,\left(\frac{r^2_0r^2_2}{r^4_{02}}\right)^{\gamma_2}\,\left(\frac{2^{-\frac{1}{2}\gamma_2}}{\Gamma\left(3/2-\gamma_2\right)}\right)^2\frac{\gamma^2_2}{r^2_0}\left\{1-\frac{2}{(3-2\,\gamma_2)}\;(\boldsymbol{Q}_T\boldsymbol{r}_0)^2\right\}$$

Integrating first over d^2r_0 we obtain

$$N^{\rm incl}_{I\!P}\left(Y,y_1,r_1,r_2,Q_T,p_{1\perp},Y_1\right) \;=\; \frac{128\,C_F}{\bar{\alpha}_S(2\pi)^4}\,r^2_1r^2_2\int_{\epsilon-i\infty}^{\epsilon+i\infty}\frac{d\gamma_1}{2\pi i}\int_{\epsilon-i\infty}^{\epsilon+i\infty}\frac{d\gamma_2}{2\pi i}\;C^2(\gamma_1)\;C^2(\gamma_2) \tag{60}$$

$$e^{\bar{\alpha}_S\left(\chi(\gamma_1)\left(\frac{1}{2}Y-y_1\right)+\chi(\gamma_2)\left(\frac{1}{2}Y+y_1\right)\right)}\,\left(\frac{1}{r^2_1\,p^2_{1\perp}}\right)^{\gamma_1}\,\left(\frac{1}{r^2_2\,p^2_{1\perp}}\right)^{\gamma_2}\,\left(\frac{2^{-\gamma_{12}}}{\Gamma\left(3/2-\gamma_1\right)^2\Gamma\left(3/2-\gamma_1\right)^2}\right)^2\,\frac{\Gamma\left(-1+\gamma_{12}\right)}{\Gamma\left(2-\gamma_{12}\right)}$$

$$\left\{1+4\;(\gamma_{12}-1)\,\gamma_{12}\left(\frac{2}{(3-2\,\gamma_1)}\;+\;\frac{2}{(3-2\,\gamma_2)}\right)\left(\frac{\boldsymbol{Q}_T\cdot\boldsymbol{p}_{1,\perp}}{p^2_{1\perp}}\right)^2\right\}$$

In Eq. (60) we denote $\gamma_{12}=\gamma_1+\gamma_2$, consider $r_0\ll r_1(r_2)$, and neglected the contributions of the order of Q^4_T.

For further estimates, we need to return to a general formula of Eq. (46). We know that as a result of the shadowing corrections $N^G\left(Y;r_\perp,r_1;b\right)\;\to\;1$ for large values of Y. It means that $\nabla^2_\perp\,N^G\left(Y;r_\perp,r_1;b\right)\;\to\;0$ in the saturation region, where $r^2_\perp Q^2_s\left(Y\right)\;\gg\;1$. Such behavior stems from the diagrams of Fig. 2-b, but not from the first diagram that we are presently considering. Consequently, we have $\nabla^2_\perp\,N^G\left(Y;r_\perp,r_1;b\right)\;\to\;0$ which vanishes both at $r^2_\perp Q^2_s\left(Y\right)\;\gg\;1$ and at $r^2_\perp Q^2_s\left(Y\right)\;\ll\;1$, and the main contribution originates for the value of r in the vicinity of the saturation scale $r^2_\perp Q^2_s\left(Y\right)\;\approx\;1$. As we have discussed, in the vicinity of the saturation scale $\gamma_1=\gamma_2=\bar{\gamma}=1-\gamma_{cr}=0.63$ (see Eq. (37) and Eq. (36)). The second observation which simplifies the estimates, is that in our approach $r_1=r_2\;\sim\;1/m$ and $m\gg m_1$ and m_2 (see Table 1). Since the typical Q_T in the integration is approximately m_1 or m_2, we can neglect the Q_T dependance of the BFKL Pomeron .

Therefore, we can write the double inclusive production cross section in the following form

$$\frac{d^2\sigma^{2\text{ parton showers}}}{dy_1\;dy_2,d^2p_{1\perp}d^2p_{2\perp}}\Bigg/\int\frac{d\phi}{2\pi}\frac{d^2\sigma^{2\text{ parton showers}}}{dy_1\;dy_2,d^2p_{1\perp}d^2p_{2\perp}}\;=\;1\;+\;\frac{\kappa}{p^2_{1\perp}\,p^2_{2\perp}}\cos\left(2\phi\right) \tag{61}$$

where κ is equal to

$$\kappa\;=\;\left(\frac{8\bar{\gamma}\left(2\bar{\gamma}-1\right)}{3-2\,\bar{\gamma}}\right)^2\,\frac{\sum^{i=2,j=2}_{i=1,j=1}\alpha^2_i\;\alpha^2_j\;g^2_i\;g^2_j\int dQ^2_T\;\frac{Q^4_T}{\left(1+Q^2_T/m^2_i\right)^2\left(1+Q^2_T/m^2_j\right)^2}}{\sum^{i=2,j=2}_{i=1,j=1}\alpha^2_i\;\alpha^2_j\;g^2_i\;g^2_j\int dQ^2_T\;\frac{1}{\left(1+Q^2_T/m^2_i\right)^2\left(1+Q^2_T/m^2_j\right)^2}} \tag{62}$$

In our model $i=j=1$ gives the largest contribution, due to large value of g_1(see Table 1), and we obtain $\kappa=0.04\,GeV^4$. The contribution of the term proportional to $\cos\left(2\phi\right)$ depends on the value of $p_\perp$. Actually, we can trust Eq. (61) for $p_{i,\perp}\;\geq\;Q_s(Y)$. Integrating over $p_{1\perp}$ and $p_{2\perp}$ we expect that the contribution to the correlation function will be equal to

$$R\left(y_1,y_2,\phi\right)\;=\;R\left(y_1,y_2\right)\left(\frac{\kappa}{Q^4_s\left(Y\right)}\right)\cos\left(2\phi\right)\;=\;2\,v^2_2\,\cos\left(2\phi\right) \tag{63}$$

leading to $R\left(\frac{1}{2}Y,\frac{1}{2}Y,\phi\right)\;=\;2\,0.06\cos\left(2\phi\right)$ for $Q_s\;\approx\;1\,GeV$ or $v_2\;=\;0.23$. This value is in a good agreement with the estimates for this correlation from the elliptic flow[70] and experimental data[71, 72]. Eq. (61) leads to $v_2=R\left(y_1,y_2\right)\kappa/p^2_{1,\perp}\,p^2_{2,\perp}$. However, we can trust this $p_\perp$ dependence only for $p^2_{1\perp}>Q_s$ and $p^2_{2\perp}>Q_s$. We should introduce the shadowing corrections to reproduce the behaviour of v_2 for $p^2_{1\perp}<Q_s$ and $p^2_{2\perp}<Q_s0$. We will do this in the next section for our model, but here we estimate the influence of the shadowing correction by integrating Eq. (59) over r_0 in the limits $0\;<\;r_0\;<\;R\sim1/Q_s$. Indeed, as has been mentioned, $N_G\to0$ for $r_0\gg1/Q_s$. In Fig. 5 we plot the v_2 dependence for $p_{1\perp}=p_{2\perp}$ for $Q_s=1\,GeV$ and choosing $R=3/Q_s$. One can see that v_2 decreases at $p_\perp<Q_s$.

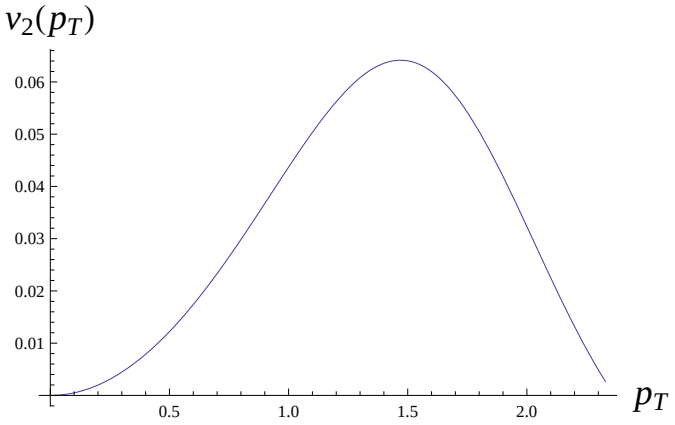

FIG. 5: $\nu_{22} \equiv v_{22}$ versus $p_T \equiv p_\perp$ for $p_{1\perp} = p_{2\perp} = p_T$. $R = 3/Q_s$ at $Q_s = 1\,GeV$.

FORMULA FOR AZIMUTHAL CORRELATIONS OF TWO PARTICLES PRODUCED IN TWO PARTON SHOWERS

Based on our experience from calculating the first diagrams, we can estimate the two particle angular correlations that stem for the general diagram of Fig. 2-b. The general formulae have the same form as Eq. (46), which we used in estimating the contribution of the first diagram. However, we now need to calculate N_G in Eq. (46) using our model described in section 2. As we have seen for angular correlations, it is essential to use the r and b dependence of the BFKL contribution. Bearing this in mind, we have to generalize Eq. (3) replacing it by the following formula

$$T\left(r_\perp, b, Y\right) \,\to\, T_W\left(r_\perp, b, Y\right) \;=\; \phi_0\,\left(w\,w^*\,Q_s^2\left(Y, b\right)\right)^{\bar{\gamma}} \tag{64}$$

where $w\,w^*$ is given by Eq. (32) with the arguments $r_2 = r_\perp = r_0$ and $r_2 = 1/m$, and Q_s is given by Eq. (4). In Eq. (64) we replace $r_\perp^2$ in Eq. (3) by $w\,w^*$, since T_W describes the behavior of the scattering amplitude in the vicinity of the saturation scale.

The expression of N_G is the direct generalization of Eq. (24) and has the following form

$$N_G^i\left(r_\perp, r_1; Y, Q_T\right) \;=\; \int d^2b\; e^{i\boldsymbol{Q}_T\cdot\boldsymbol{b}}\; N^{\rm BK}\left(\int d^2b'\, G^{\rm dressed}\Big(T_W\left(r_\perp, b', Y\right)\Big) g_i\left(\boldsymbol{b}-\boldsymbol{b}'\right)\right) \tag{65}$$

Calculating $\nabla^2_{r_\perp} N_G^i\left(r_\perp, r_1; Y, Q_T\right)$ we see that we have two contributions

$$\begin{aligned}
&\nabla^2_{r_\perp} N_G^i\left(r_\perp, r_1; Y, Q_T\right) \;=\; \int d^2b\, d^2b'\;\; e^{i\boldsymbol{Q}_T\cdot\boldsymbol{b}} \qquad (66)\\
&\left\{\nabla^2_{r_\perp}\, G^{\rm dressed}\Big(T_W\left(r_\perp, b', Y\right)\Big)\frac{d}{dG^{\rm dressed}} \;+\; \boldsymbol{\nabla}_{r_\perp} G^{\rm dressed}\Big(T_W\left(r_\perp, b', Y\right)\Big)\cdot\boldsymbol{\nabla}_{r_\perp} G^{\rm dressed}\Big(T_W\left(r_\perp, b', Y\right)\Big)\frac{d^2}{\left(dG^{\rm dressed}\right)^2}\right\}\\
&N^{\rm BK}\left(\int d^2b'\, G^{\rm dressed}\Big(T_W\left(r_\perp, b', Y\right)\Big) g_i\left(\boldsymbol{b}-\boldsymbol{b}'\right)\right)
\end{aligned}$$

The first term in Eq. (66) is proportional to $\left(r_\perp^2\right)^{\bar{\gamma}-2}$, while the second one is $\propto \left(r_\perp^2\right)^{2\bar{\gamma}-2}$. Therefore, for small $r_\perp$ we can neglect the second term.

We have that

$$\begin{aligned}
&\frac{d}{dG^{\rm dressed}} N^{\rm BK}\left(\int d^2b'\, G^{\rm dressed}\Big(T_W\left(r_\perp, b', Y\right)\Big) g_i\left(\boldsymbol{b}-\boldsymbol{b}'\right)\right) \;= \qquad (67)\\
&\qquad g_i\left(\boldsymbol{b}-\boldsymbol{b}'\right)\frac{dN^{\rm BK}\left(\mathcal{Z}\right)}{d\mathcal{Z}}\left(\mathcal{Z} = \int d^2b'\, G^{\rm dressed}\Big(T_W\left(r_\perp, b', Y\right)\Big) g_i\left(\boldsymbol{b}-\boldsymbol{b}'\right)\right)
\end{aligned}$$

with

$$N'^{\rm BK}\left(\mathcal{Z}\right) \equiv \frac{dN^{\rm BK}\left(\mathcal{Z}\right)}{d\mathcal{Z}} \;=\; a\, e^{-\mathcal{Z}} \,+\, \frac{1-a}{\left(1\,+\,\mathcal{Z}\right)^2} \tag{68}$$

For small $r_\perp$

$$\begin{aligned}\nabla^2_{r_\perp} G^{\rm dressed}\Big(T_W\left(r_\perp, b', Y\right)\Big) \;&=\; \nabla^2_{r_\perp} T_W\left(r_\perp, b', Y\right)\, \frac{d}{dT} G^{\rm dressed}\Big(T = T_W\left(r_\perp, b', Y\right)\Big) \\ &\equiv\; \underbrace{\nabla^2_{r_\perp} N_{I\!P}\left(r_\perp, b', Y\right)}_{r_{bot}\to 1/Q_s(Y,b)}\, \frac{d}{dT} G^{\rm dressed}\Big(T = T_W\left(r_\perp, b', Y\right)\Big)\end{aligned} \tag{69}$$

with

$$G'\left(T\right) \equiv \frac{d}{dT} G^{\rm dressed}\left(T\right) \;=\; a^2 e^{-T} + \frac{(a-1)^2 e^{1/T}(T+1)\Gamma\left(0, \frac{1}{T}\right)}{T^3} + (a-1)\left(\frac{1-a}{T^2} - \frac{2a}{(T+1)^2}\right) \tag{70}$$

Plugging Eq. (67) - Eq. (70) into Eq. (66) and using that $b' \approx 1/m \ll\ b \approx 1/m_i$ we obtain

$$\nabla^2_{r_\perp} N^i_G\left(r_\perp, r_1; Y, Q_T\right) \;=\; \underbrace{\nabla^2_{r_\perp} N^i_G\left(r_\perp, Y, Q_T\right)}_{r_\perp \to 1/Q_s}\, \widetilde{G'}\left(r_\perp, Y\right)\, N'^{\rm BK}_i\left(r_\perp, Y, Q_T\right) \tag{71}$$

$$N'^{\rm BK}_i\left(r_\perp, Y, Q_T\right) \;=\; \int d^2b\, e^{i\boldsymbol{Q}_T\cdot\boldsymbol{b}}\, g_i\left(b\right)\, N'^{\rm BK}\Big(\widetilde{G}\left(r_\perp, Y\right)\, g_i\left(b\right)\Big)$$

where

$$\begin{aligned}\widetilde{G}\left(r_\perp, Y\right) \;&=\; \int d^2b'\, G\Big(T\left(r_\perp, b', Y\right)\Big) \\ \widetilde{G'}\left(r_\perp, Y\right) \;&=\; \int d^2b'\, S(b', m)\, G'\Big(T\left(r_\perp, b', Y\right)\Big)\end{aligned} \tag{72}$$

Using Eq. (57), in which we substitute $\gamma = \bar{\gamma}$ we obtain

$$\begin{aligned}&\nabla^2_\perp N^i_G\left(Y; r_\perp; Q_T\right) \;\to\; 4\, C^2(\bar{\gamma})\, r^2_{01}\, e^{\bar{\alpha}_S\,\chi(\bar{\gamma})\,Y} \\ &\times\; \left(\frac{r^2_\perp r^2_1}{r^4_{01}}\right)^{\bar{\gamma}} \left(\frac{2^{-\frac{1}{2}\bar{\gamma}}}{\Gamma\left(3/2-\bar{\gamma}\right)}\right)^2 \frac{\bar{\gamma}^2}{r^2}\Bigg\{1 - \frac{2}{(3-2\,\bar{\gamma})}\, \left(\boldsymbol{Q}_T \boldsymbol{r}_\perp\right)^2\Bigg\} \widetilde{G'}\left(r_\perp, Y\right)\, N'^{\rm BK}_i\left(r_\perp, Y, Q_T\right) \\ &=\; \mathcal{C}\left(\bar{\gamma}\right)\, e^{\bar{\alpha}_S\,\chi(\bar{\gamma})\,Y}\, r^2_{01} \left(\frac{r^2_\perp r^2_1}{r^4_{01}}\right)^{\bar{\gamma}} \frac{1}{r^2_\perp}\Bigg\{1 - \frac{2}{(3-2\,\bar{\gamma})}\, \left(\boldsymbol{Q}_T \boldsymbol{r}_\perp\right)^2\Bigg\} \widetilde{G'}\left(r_\perp, Y\right)\, N'^{\rm BK}_i\left(r_\perp, Y, Q_T\right)\end{aligned} \tag{73}$$

Using Eq. (73) we can re-write the double inclusive cross section in the form (see Eq. (61))

$$\frac{d^2\sigma^{2\text{ parton showers}}}{dy_1\; dy_2, d^2p_{1\perp} d^2p_{2\perp}} \Bigg/ \int \frac{d\phi}{2\pi} \frac{d^2\sigma^{2\text{ parton showers}}}{dy_1\; dy_2, d^2p_{1\perp} d^2p_{2\perp}} \;=\; 1 \;+\; 2v_{22}\left(p_{1T}, p_{2T}\right) \cos\left(2\phi\right) \tag{74}$$

where

$$v_{22}\left(p_{1T}, p_{2T}\right) \;=\; N\left(p_{1\perp}, p_{2\perp}, Y\right) \Big/ D\left(p_{1\perp}, p_{2\perp}, Y\right) \tag{75}$$

where

$$\begin{aligned}&N\left(p_{1\perp}, p_{2\perp}, Y, y_1, y_2\right) \;= \\ &\frac{1}{4} \sum_{i=1,j=1}^{i,j} \alpha^2_i \alpha^2_j \Bigg\{ \int \frac{dr^2_\perp}{r^2_\perp} J_2\left(p_{1\perp} r_\perp\right) \left(\frac{r^2_\perp}{r^2_1}\right)^{2\bar{\gamma}} \frac{4}{(3-2\,\bar{\gamma})} \widetilde{G'}\left(r_\perp, \frac{1}{2}Y - y_1\right)\, \widetilde{G'}\left(r_\perp, \frac{1}{2}Y + y_1\right) \Bigg\} \\ \times\; &\left\{ \int \frac{dr'^2_\perp}{r'^2_\perp} J_2\left(p_{1\perp} r'_\perp\right) \left(\frac{r'^2_\perp}{r^2_1}\right)^{2\bar{\gamma}} \frac{4}{(3-2\,\bar{\gamma})} \widetilde{G'}\left(r'_\perp, \frac{1}{2}Y - y_2\right)\, \widetilde{G'}\left(r'_\perp, \frac{1}{2}Y + y_2\right) \right\} \int dQ^2_T\; Q^4_T \\ &N'^{\rm BK}_i\left(r_\perp, \frac{1}{2}Y - y_1, Q_T\right)\, N'^{\rm BK}_j\left(r_\perp, \frac{1}{2}Y + y_1, Q_T\right)\, N'^{\rm BK}_i\left(r'_\perp, \frac{1}{2}Y - y_2, Q_T\right)\, N'^{\rm BK}_j\left(r'_\perp, \frac{1}{2}Y + y_2, Q_T\right)\end{aligned} \tag{76}$$

and

$$
\begin{aligned}
& D\left(p_{1\perp}, p_{2\perp}, Y, y_1, y_2\right) \; = \\
& \sum_{i=1,j=1}^{i,j} \alpha_i^2 \alpha_j^2 \left\{ \int \frac{dr_\perp^2}{r_\perp^4} J_0\left(p_{1\perp} r_\perp\right) \left(\frac{r_\perp^2}{r_1^2}\right)^{2\bar{\gamma}} \widetilde{G'}\left(r_\perp, \frac{1}{2}Y - y_1\right) \widetilde{G'}\left(r_\perp, \frac{1}{2}Y + y_1\right) \right\} \\
\times \; & \left\{ \int \frac{dr_\perp'^2}{r_\perp'^4} J_0\left(p_{1\perp} r'_\perp\right) \left(\frac{r_\perp'^2}{r_1^2}\right)^{2\bar{\gamma}} \widetilde{G'}\left(r'_\perp, \frac{1}{2}Y - y_2\right) \widetilde{G'}\left(r_\perp, \frac{1}{2}Y + y_2\right) \right\} \int dQ_T^2 \\
& N_i'^{\rm BK}\left(r_\perp, \frac{1}{2}Y - y_1, Q_T\right) N_j'^{\rm BK}\left(r_\perp, \frac{1}{2}Y + y_1, Q_T\right) N_i'^{\rm BK}\left(r'_\perp, \frac{1}{2}Y - y_2, Q_T\right) N_j'^{\rm BK}\left(r'_\perp, \frac{1}{2}Y + y_2, Q_T\right)
\end{aligned}
\tag{77}
$$

DOUBLE INCLUSIVE CROSS SECTION IN THE EVENTS WITH FIXED MULTIPLICITY

In this section we calculate the angular dependance of the double inclusive cross section, for the event with large multiplicity. In our approach, the large multiplicity event stems from the production of several parton showers, as it is shown in Fig. 6 . Indeed, if N particles are produced in the collision, the n parton showers contribute, where $n = N/\bar{n}$. $\bar{n}$ is the multiplicity in the single parton shower, which can be estimated as being equal to the average multiplicity in the single inclusive production. Bearing this in mind, we see that

$$
\begin{aligned}
& \frac{d^2\sigma}{dy_1 dy_2 d^2p_{1T} d^2p_{2T}} \; = \\
& n \frac{d^2\sigma^{\text{one parton shower}}}{dy_1 dy_2 d^2p_{1T} d^2p_{2T}} \; + \; n(n-1) \frac{d^2\sigma^{\text{two parton showers}}}{dy_1 dy_2 d^2p_{1T} d^2p_{2T}} \Big(1 \, + \, \mathcal{R}\left(p_{1T}, p_{2T}\right) \cos\left(2\phi\right) \Big)
\end{aligned}
\tag{78}
$$

The calculation of the first term in Eq. (83) can be simplified for $y_1 \approx y_2$ by using the following relation (see Ref.[73])

$$
\frac{d\sigma}{dy d^2p_T} \; = \; \frac{8\,C_F}{\alpha_S\left(2\,\pi\right)^4} \frac{1}{p_T^2} F^{\rm incl}\left(p_T\right); \quad \frac{d^2\sigma^{\text{one parton shower}}}{dy_1 dy_2 d^2p_{1T} d^2p_{2T}}|_{y_1 = y_2} \; = \; \Big(\frac{8\,C_F}{\alpha_S\left(2\,\pi\right)^4}\Big)^2 \frac{1}{p_{1T}^2\, p_{2T}^2} F^{\rm incl}\left(|\boldsymbol{p}_{1T} + \boldsymbol{p}_{2T}|\right) \tag{79}
$$

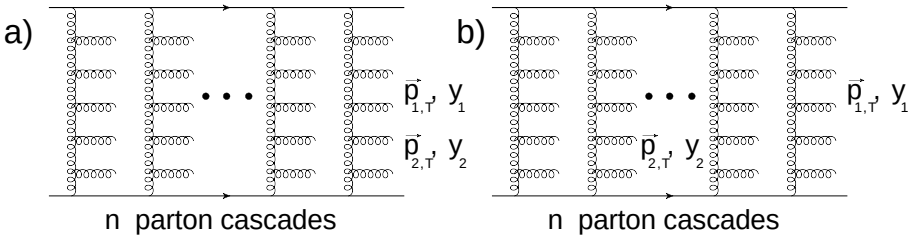

FIG. 6: The large multiplicity event in our approach: production from one parton shower (Fig. 6-a) and from two parton showers (Fig. 6-b).

The expression for the function $F^{\rm incl}$ we have found and it is equal to

$$
\begin{aligned}
& F_{i,j}^{\rm incl}\left(p_T, Y, y_1\right) \; = \; \int \frac{dr_\perp^2}{r_\perp^4} J_0\left(p_{1\perp} r_\perp\right) \left(\frac{r_\perp^2}{r_1^2}\right)^{2\bar{\gamma}} \\
& \times \widetilde{G'}\left(r_\perp, \frac{1}{2}Y - y_1\right) \widetilde{G'}\left(r_\perp, \frac{1}{2}Y + y_1\right) N_i'^{\rm BK}\left(r_\perp, \frac{1}{2}Y - y_1, Q_T = 0\right) N_j'^{\rm BK}\left(r_\perp, \frac{1}{2}Y + y_1, Q_T = 0\right)
\end{aligned}
\tag{80}
$$

Therefore, the first term in Eq. (83) reduces to the following expression

$$
n \frac{d^2\sigma_{i,j}^{\text{one parton shower}}}{dy_1 dy_2 d^2p_{1T} d^2p_{2T}} \; = \; n \Big(\frac{8\,C_F}{\alpha_S\left(2\,\pi\right)^4}\Big)^2 \frac{1}{p_{1T}^2\, p_{2T}^2} F_{i,j}^{\rm incl}\left(|\boldsymbol{p}_{1T} + \boldsymbol{p}_{2T}|\right) \tag{81}
$$

where $F_{i,j}^{\rm incl}$ is given by Eq. (80).

The second term in Eq. (83) is almost equal to Eq. (77)

$$
\begin{aligned}
n(n-1)\frac{d^2\sigma_{i,j}^{\text{two parton showers}}}{dy_1 dy_2 d^2p_{1T} d^2p_{2T}} \;&=\; n\,(n-1)\left(\frac{8\,C_F}{\alpha_S\,(2\,\pi)^4}\right)^2 \frac{1}{p_{1T}^2\,p_{2T}^2} \qquad (82)\\
&\left\{\int \frac{dr_\perp^2}{r_\perp^4} J_0\left(p_{1\perp} r_\perp\right)\left(\frac{r_\perp^2}{r_1^2}\right)^{2\bar{\gamma}} \widetilde{G'}\left(r_\perp, \frac{1}{2}Y - y_1\right)\widetilde{G'}\left(r_\perp, \frac{1}{2}Y + y_1\right)\right\}\\
\times\;&\left\{\int \frac{dr_\perp'^2}{r_\perp'^4} J_0\left(p_{1\perp} r'_\perp\right)\left(\frac{r_\perp'^2}{r_1^2}\right)^{2\bar{\gamma}} \widetilde{G'}\left(r'_\perp, \frac{1}{2}Y - y_2\right)\widetilde{G'}\left(r_\perp, \frac{1}{2}Y + y_2\right)\right\}\int dQ_T^2\\
&N_i'^{\text{BK}}\left(r_\perp, \frac{1}{2}Y - y_1, Q_T\right) N_j'^{\text{BK}}\left(r_\perp, \frac{1}{2}Y + y_1, Q_T\right) N_i'^{\text{BK}}\left(r'_\perp, \frac{1}{2}Y - y_2, Q_T\right) N_j'^{\text{BK}}\left(r'_\perp, \frac{1}{2}Y - y_2, Q_T\right)
\end{aligned}
$$

Using our calculation for inclusive production[13], and for the rapidity correlation function we can re-write Eq. (82) in the form

$$
\begin{aligned}
\frac{1}{\sigma_{in}}\frac{d^2\sigma}{dy_1 dy_2 d^2p_{1T} d^2p_{2T}} \;&=\; n\Big(\frac{8\,C_F}{\alpha_S\,(2\,\pi)^4}\Big)\,\frac{1}{\sigma_{in}}\frac{d\sigma}{dy_1}\frac{1}{p_{1T}^2\,p_{2T}^2}\,\frac{\sum_{i=1,j=1}^{i=2,j=2}\alpha_i^2\,\alpha_j^2\,F_{i,j}^{\text{incl}}\left(|\boldsymbol{p}_{1T}+\boldsymbol{p}_{2T}|\right)}{\sum_{i=1,j=1}^{i=2,j=2}\alpha_i^2\,\alpha_j^2\int\frac{d^2p_T}{p_T^2}F_{i,j}^{\text{incl}}\left(p_T\right)}\\
&+\;\frac{n(n-1)}{2}\frac{1}{\sigma_{in}}\frac{d\sigma}{dy_1}\frac{1}{\sigma_{in}}\frac{d\sigma}{dy_2}\Big(1\;+\;R\left(y_1,y_2\right)\Big)\Big(1\;+\;2v_{22}\left(p_{1T},p_{2T}\right)\,\cos\left(2\phi\right)\Big)\\
&\sum_{i=1,j=1}^{i=2,j=2}\alpha_i^2\,\alpha_j^2\,\frac{d^2\sigma_{i,j}^{\text{two parton showers}}}{dy_1 dy_2 d^2p_{1T} d^2p_{2T}}\Bigg/\sum_{i=1,j=1}^{i=2,j=2}\alpha_i^2\,\alpha_j^2\int d^2p_{1T}\,d^2p_{2T}\frac{d^2\sigma_{i,j}^{\text{two parton showers}}}{dy_1 dy_2 d^2p_{1T} d^2p_{2T}} \qquad (83)
\end{aligned}
$$

PREDICTIONS AND COMPARISON WITH THE EXPERIMENT

Eq. (83) has the form that has been used in the analysis of the experimental data[72]: viz.

$$
\begin{aligned}
&\int dy_1 dy_2 \int_{p_{1T}^{min}}^{p_{1T}^{max}} dp_{1T}\int_{p_{2T}^{min}}^{p_{2T}^{max}} dp_{2T}\frac{1}{\sigma_{in}}\frac{d^2\sigma}{dy_1 dy_2 dp_{1T} dp_{2T}\,d\phi} \equiv \qquad (84)\\
&\int dy_1 dy_2 \int_{p_{1T}^{min}}^{p_{1T}^{max}} dp_{1T}\int_{p_{2T}^{min}}^{p_{2T}^{max}} dp_{2T}\frac{d^2N}{dy_1 dy_2 dp_{1T} dp_{2T}\,d\phi} \;=\; Y^{\text{periph}}\left(\phi\right)\;+\;Y^{\text{ridge}}\left(\phi\right)
\end{aligned}
$$

where ϕ denotes the difference between the azimuthal angles $\phi = \phi_1 - \phi_2$.

$Y^{\text{periph}}\left(\phi\right)$ describes the production of two gluons from one parton shower (see Fig. 6-a) while $Y^{\text{ridge}}\left(\phi\right)$ stands for the second term, which is related to the emission of gluons from two different parton showers (see Fig. 6-b). Eq. (83) shows several qualitative features which have been observed experimentally [71, 72]: (1) $Y^{\text{periph}}\left(\phi\right)$ is smaller than $Y^{\text{ridge}}\left(\phi\right)$ and (2) it decreases with increasing multiplicity of the event; (their ratio is proportional to 1/n); and (3) v_{22} does not depend on the multiplicity of the event and on the rapidity difference $Y_{12} = Y_1 - Y_2$.

From Eq. (76) and Eq. (77) we can see that

$$
\begin{aligned}
N\;&\propto\;\int d^2Q_T\,Q_T^4\left(\int\frac{d^2r_\perp}{r_\perp^2}J_2\left(p_{1T}r_\perp\right)N_{ij}\left(r_\perp,Q_T\right)\right)\left(\int\frac{d^2r'_\perp}{r'^2_\perp}J_2\left(p_{2T}r'_\perp\right)N_{ij}\left(r'_\perp,Q_T\right)\right);\\
D\;&\propto\;\int d^2Q_T\,\left(\int\frac{d^2r_\perp}{r_\perp^4}J_0\left(p_{1T}r_\perp\right)N_{ij}\left(r_\perp,Q_T\right)\right)\left(\int\frac{d^2r'_\perp}{r'^4_\perp}J_0\left(p_{2T}r'_\perp\right)N_{ij}\left(r'_\perp,Q_T\right)\right); \qquad (85)
\end{aligned}
$$

As we have discussed, functions $N_{i,j}$ have maxima at $r_\perp \approx 1/Q_s$. In Fig. 7 we plot function N_{11} at W = 13 TeV. One can see that N_{11} has a maximum at $r_\perp \approx 3 \div 4\,GeV^{-1}$. Therefore, our estimates in section 4.2 are justified.

The calculations of v_{22} using Eq. (75) with the parameters of Table 1, are shown in Fig. 8. In Eq. (84) we integrate over p_{2T} in the intervals shown in the figure: $0.5 \div 1\,GeV$, $2 \div 3\,GeV$ and $0.5 \div 5\,GeV$.

First conclusion from these figures is that v_{22} does not depend on energy, which is in agreement with the experimental data of Ref.[72]. . The values of $v_2(p_T)$ which is determined as

$$
v_2\left(p_{1T}\right) \;=\; \frac{v_{22}\left(p_{1T},p_{2T}\right)}{\sqrt{v_{22}\left(p_{2T},p_{2T}\right)}} \qquad (86)
$$

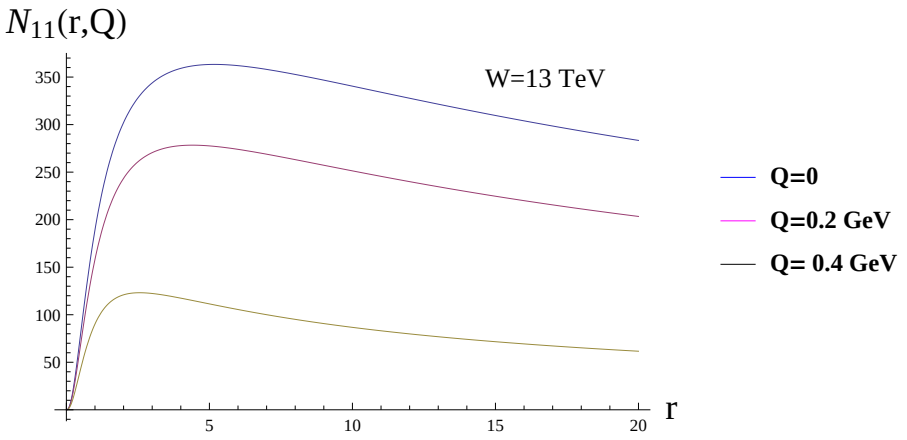

FIG. 7: N_{11} of Eq. (85) versus $r_\perp$ at different values of $Q \equiv Q_T$.

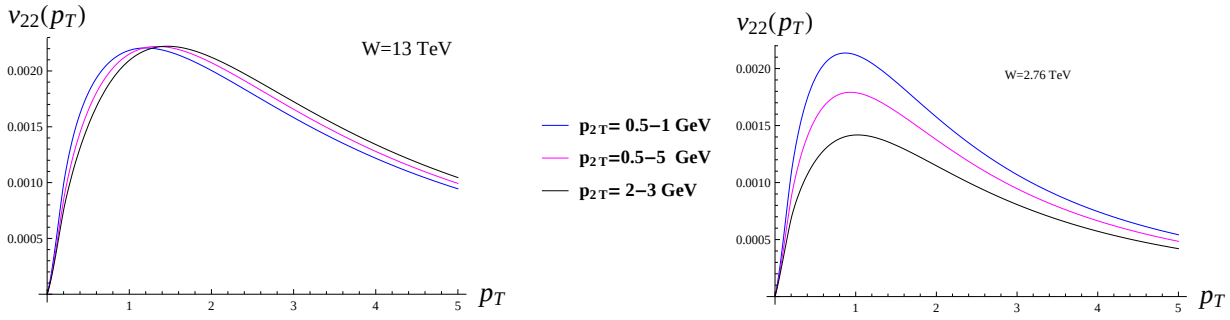

Fig. 8-a

Fig. 8-b

FIG. 8: $\nu_{22} \equiv v_{22}$ versus p_T at W = 13 TeV (Fig. 8-a) and at W = 2.76 TeV (Fig. 8-b).

are plotted in Fig. 9.

Comparing this figure with the experimental measurements of ATLAS [72] we see: (1) that the p_T distribution for calculated v_2, is narrower than the experimental one; (2) it has a peak at $p_T = 0.5 \div 1.5\, GeV$ while the experimental distribution has a maximum at $p_T = 2 \div 3\, GeV$ and (3) the magnitude of v_2 is about 0.6-0.7 of the experimental one (see Fig. 10).

In our calculation, we used Eq. (5) for the saturation scale of Eq. (4). This equation gives a natural generalization of our description of the diffractive processes using only one parameter, m^2. However, we can introduce a different scale:

$$Q_{0s}^2\left(b, Y_0\right) \;=\; Q_0^2 \left(\frac{1}{m^2} S\left(b, m\right)\right)^{\frac{1}{\gamma}} \tag{87}$$

and view Q_0 as a new fitting parameter. In Fig. 11 we plot the value of v_2 for $Q_0 = 0.2m$. This choice does not change the character of p_T dependence, but leads to a larger value than our previous estimates.

Therefore, from comparison with the experiment data, we can conclude that the density variation mechanism in the framework of CGC/saturation approach, gives a substantial contribution which cannot be neglected.

CONCLUSION

In this paper we estimate the contribution of the density variation mechanism to the value of v_2. This was done in a model based on CGC/saturation approach. It has been demonstrated in Refs.[11–14], that the model is able to describe both the diffraction-type reactions (the total and inelastic cross section, elastic cross section and its t distribution, diffractive production) and the multi-particle production processes, such as inclusive cross sections

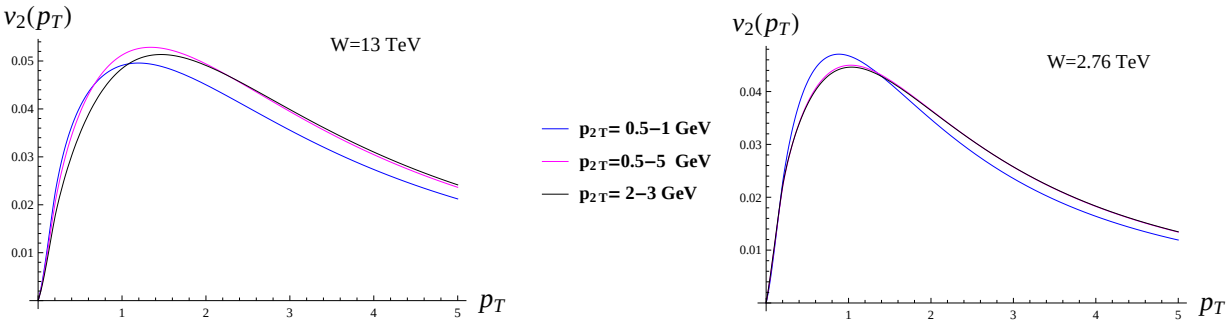

Fig. 9-a Fig. 9-b

FIG. 9: $\nu_2 \equiv v_2$ versus p_T at W = 13 TeV (Fig. 9-a) and at W = 2.76 TeV (Fig. 9 - b).

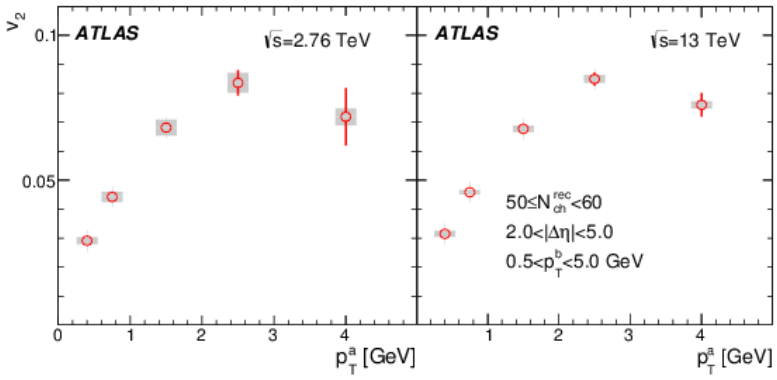

FIG. 10: v_2 versus p_T at W = 2.76 TeV and at W = 13 TeV. The figure is taken from Ref.[72]

and rapidity correlations. We present here, the first attempt to describe the azimuthal angular correlation, in the framework of a unique approach based on an effective theory for high energy QCD.

Comparing with the experimental v_2 in proton-proton collision, we conclude that the density variation mechanism in the framework of CGC/saturation approach, provides a substantial contribution which cannot be neglected. Bearing in mind that in CGC/saturation approach there are other two mechanisms present: Bose enhancement in the wave function[50] and local anisotropy[51, 52], we believe that the azimuthal long range rapidity correlations in proton-proton collisions stem from the CGC/saturation physics, and not from quark-gluon plasma production. It should be noted that none of the models based on the quark-gluon plasma production are able to describe diffractive physics. Hence, at present, the CGC/saturation approach, appears to be the only effective theory that can provide such a description.

We plan to include other CGC sources in the description of v_2, as well as compare in more detail, the cross section for double inclusive production of two gluon jets in proton-proton collisions.

ACKNOWLEDGEMENTS

We thank our colleagues at Tel Aviv university and UTFSM for encouraging discussions. Our special thanks go to Gideon Bella and Carlos Cantreras for elucidating discussions on the subject of this paper. This research was supported by the BSF grant 2012124 and by the Fondecyt (Chile) grant 1140842.

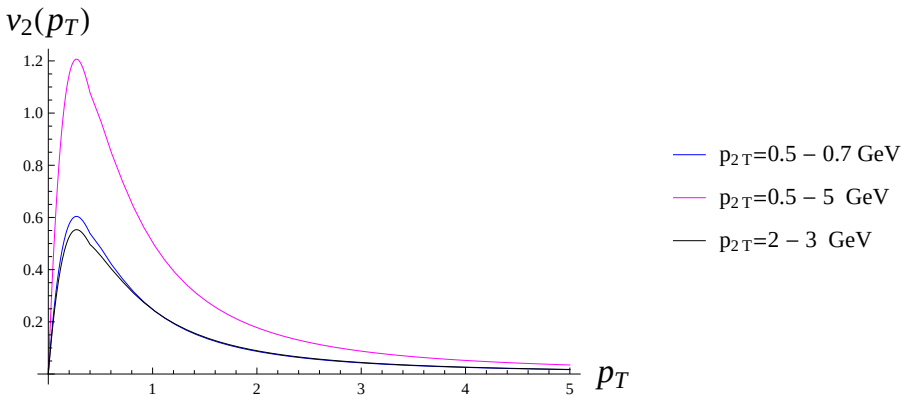

FIG. 11: v_2 versus p_T at W = 13 TeV with the choice $Q_0 = 0.2m$ in Eq. (87).

* Electronic address: gotsman@post.tau.ac.il
† Electronic address: leving@post.tau.ac.il, eugeny.levin@usm.cl
‡ Electronic address: maor@post.tau.ac.il
§ Electronic address: sebastian.tapia.aray@cern.ch

[1] M. G. Poghosyan, J. Phys. G G **38**, 124044 (2011) [arXiv:1109.4510 [hep-ex]]. ALICE Collaboration, *"First proton–proton collisions at the LHC as observed with the ALICE detector: measurement of the charged particle pseudorapidity density at $\sqrt{s}$ = 900 GeV,"* arXiv:0911.5430 [hep-ex]; A. R. Timmins [ALICE Collaboration], J. Phys. G **38** (2011) 124093; A. R. Timmins [ALICE Collaboration], arXiv:1106.6057 [nucl-ex]; J. Phys. G **38** (2011) 124091 [arXiv:1107.0285 [nucl-ex]].
[2] G. Aad *et al.* [ATLAS Collaboration], Nature Commun. **2**, 463 (2011) [arXiv:1104.0326 [hep-ex]].
[3] CMS Physics Analysis Summary: "Measurement of the inelastic pp cross section at $\sqrt{s} = 7$ TeV with the CMS detector", 2011/08/27.
[4] F. Ferro [TOTEM Collaboration], AIP Conf. Proc. **1350**, 172 (2011) ; G. Antchev *et al.* [TOTEM Collaboration], Europhys. Lett. **96**, 21002 (2011), **95**, 41001 (2011) [arXiv:1110.1385 [hep-ex]]; G. Antchev *et al.* [TOTEM Collaboration], Phys. Rev. Lett. **111** (2013) 26, 262001 [arXiv:1308.6722 [hep-ex]].
[5] ALICE Collaboration, Eur. Phys. J. C **65** (2010) 111 [arXiv:0911.5430 [hep-ex]].
[6] S. Chatrchyan *et al.* [CMS and TOTEM Collaborations], Eur. Phys. J. C **74** (2014) 10, 3053 [arXiv:1405.0722 [hep-ex]]; V. Khachatryan *et al.* [CMS Collaboration], JHEP **1002** (2010) 041 [arXiv:1002.0621 [hep-ex]].
[7] ATLAS Collaboration, arXiv:1003.3124 [hep-ex].
[8] V. Khachatryan *et al.* [CMS Collaboration], JHEP **1101** (2011) 079 [arXiv:1011.5531 [hep-ex]].
[9] G. Aad *et al.* [ATLAS Collaboration], JHEP **1207** (2012) 019 [arXiv:1203.3100 [hep-ex]].
[10] Yuri V Kovchegov and Eugene Levin, *" Quantum Choromodynamics at High Energies"*, Cambridge Monographs on Particle Physics, Nuclear Physics and Cosmology, Cambridge University Press, 2012 .
[11] E. Gotsman, E. Levin and U. Maor, Eur. Phys. J. C **75** (2015) 1, 18 [arXiv:1408.3811 [hep-ph]].
[12] E. Gotsman, E. Levin and U. Maor, Eur. Phys. J. C **75** (2015) 5, 179 [arXiv:1502.05202 [hep-ph]].
[13] E. Gotsman, E. Levin and U. Maor, Phys. Lett. B **746** (2015) 154 [arXiv:1503.04294 [hep-ph]].
[14] E. Gotsman, E. Levin and U. Maor, Eur. Phys. J. C **75** (2015) 11, 518 [arXiv:1508.04236 [hep-ph]].
[15] E. Gotsman, E. Levin and U. Maor, arXiv:1510.07249 [hep-ph].
[16] L. V. Gribov, E. M. Levin and M. G. Ryskin, Phys. Rep. **100** (1983) 1.
[17] A. H. Mueller and J. Qiu, Nucl. Phys. **B268** (1986) 427.
[18] L. McLerran and R. Venugopalan, Phys. Rev. **D49** (1994) 2233, 3352; **D50** (1994) 2225; **D53** (1996) 458; **D59** (1999) 09400.
[19] I. Balitsky, [arXiv:hep-ph/9509348]; *Phys. Rev.* **D60**, 014020 (1999) [arXiv:hep-ph/9812311].
[20] A. H. Mueller, Nucl. Phys. **B415** (1994) 373; **B437** (1995) 107.
[21] Y. V. Kovchegov, *Phys. Rev.* **D60**, 034008 (1999), [arXiv:hep-ph/9901281].
[22] J. Jalilian-Marian, A. Kovner, A. Leonidov and H. Weigert, *Phys. Rev.* **D59**, 014014 (1999), [arXiv:hep-ph/9706377]; *Nucl. Phys.* **B504**, 415 (1997), [arXiv:hep-ph/9701284]; J. Jalilian-Marian, A. Kovner and H. Weigert, *Phys. Rev.* **D59**, 014015 (1999), [arXiv:hep-ph/9709432]; A. Kovner, J. G. Milhano and H. Weigert, *Phys. Rev.* **D62**, 114005 (2000), [arXiv:hep-ph/0004014] ; E. Iancu, A. Leonidov and L. D. McLerran, *Phys. Lett.* **B510**, 133 (2001); [arXiv:hep-ph/0102009]; *Nucl. Phys.* **A692**, 583 (2001), [arXiv:hep-ph/0011241]; E. Ferreiro, E. Iancu, A. Leonidov and L. McLerran, *Nucl. Phys.* **A703**, 489 (2002), [arXiv:hep-ph/0109115]; H. Weigert, *Nucl. Phys.* **A703**, 823 (2002),

[arXiv:hep-ph/0004044].
[23] E. A. Kuraev, L. N. Lipatov, and F. S. Fadin, *Sov. Phys. JETP* **45**, 199 (1977); Ya. Ya. Balitsky and L. N. Lipatov, *Sov. J. Nucl. Phys.* **28**, 22 (1978).
[24] L. N. Lipatov, Phys. Rep. **286** (1997) 131; Sov. Phys. JETP **63** (1986) 904 and references therein.
[25] A. H. Mueller and B. Patel, Nucl. Phys. **B425** (1994) 471.
[26] J. Bartels, M. Braun and G. P. Vacca, Eur. Phys. J. **C40** (2005) 419 [arXiv:hep-ph/0412218]. J. Bartels and C. Ewerz, JHEP **9909** 026 (1999) [arXiv:hep-ph/9908454]. J. Bartels and M. Wusthoff, Z. Phys. **C6**, (1995) 157. J. Bartels, Z. Phys. **C60** (1993) 471.
[27] M. A. Braun, Phys. Lett. **B632** (2006) 297 [arXiv:hep-ph/0512057]; Eur. Phys. J. **C16** (2000) 337 [arXiv:hep-ph/0001268]; Phys. Lett. **B483** (2000) 115 [arXiv:hep-ph/0003004]; Eur. Phys. J. **C33** (2004) 113 [arXiv:hep-ph/0309293]; **C6**, 321 (1999) [arXiv:hep-ph/9706373]. M. A. Braun and G. P. Vacca, Eur. Phys. J. **C6** (1999) 147 [arXiv:hep-ph/9711486].
[28] Y. V. Kovchegov and E. Levin, Nucl. Phys. B **577** (2000) 221 [hep-ph/9911523].
[29] E. Levin and M. Lublinsky, Nucl. Phys. A **763** (2005) 172 [arXiv:hep-ph/0501173]; Phys. Lett. B **607** (2005) 131 [arXiv:hep-ph/0411121]; Nucl. Phys. A **730** (2004) 191 [arXiv:hep-ph/0308279].
[30] E. Levin, J. Miller and A. Prygarin, Nucl. Phys. **A806** (2008) 245, [arXiv:0706.2944 [hep-ph]].
[31] T. Altinoluk, C. Contreras, A. Kovner, E. Levin, M. Lublinsky and A. Shulkim, Int. J. Mod. Phys. Conf. Ser. **25** (2014) 1460025; T. Altinoluk, N. Armesto, A. Kovner, E. Levin and M. Lublinsky, JHEP **1408** (2014) 007; T. Altinoluk, A. Kovner, E. Levin and M. Lublinsky, JHEP **1404** (2014) 075 [arXiv:1401.7431 [hep-ph]].; T. Altinoluk, C. Contreras, A. Kovner, E. Levin, M. Lublinsky and A. Shulkin, JHEP **1309** (2013) 115.
[32] E. Levin, JHEP **1311** (2013) 039 [arXiv:1308.5052 [hep-ph]].
[33] D. Kharzeev, E. Levin and M. Nardi, Nucl. Phys. A **730** (2004) 448 [Erratum-ibid. A **743** (2004) 329] [arXiv:hep-ph/0212316]; Phys. Rev. C **71** (2005) 054903 [arXiv:hep-ph/0111315]; D. Kharzeev and E. Levin, Phys. Lett. B **523** (2001) 79 [arXiv:nucl-th/0108006]; D. Kharzeev and M. Nardi, Phys. Lett. B **507** (2001) 121 [arXiv:nucl-th/0012025].
[34] D. Kharzeev, E. Levin and M. Nardi, Nucl. Phys. A **747** (2005) 609 [arXiv:hep-ph/0408050].
[35] E. Levin and A. H. Rezaeian, AIP Conf. Proc. **1350** (2011) 243 [arXiv:1011.3591 [hep-ph]]; Phys. Rev. D **82** (2010) 014022 [arXiv:1005.0631 [hep-ph]]; [arXiv:1102.2385 [hep-ph]]; *Phys. Rev* **D82** (2010) 054003. [arXiv:1007.2430 [hep-ph]].
[36] E. Levin and A. H. Rezaeian, Phys. Rev. D **84**, 034031 (2011) [arXiv:1105.3275 [hep-ph]].
[37] L. McLerran, M. Praszalowicz, Nucl. Phys. A **916** (2013) 210 [arXiv:1306.2350 [hep-ph]]; *Acta Phys. Polon.* **B42** (2011) 99 [arXiv:1011.3403 [hep-ph]]; *Acta Phys. Polon.* **B41** (2010) 1917. [arXiv:1006.4293 [hep-ph]].
[38] M. Praszalowicz, Phys. Lett. B **727** (2013) 461 [arXiv:1308.5911 [hep-ph]]; Acta Phys. Polon. Supp. **6** (2013) 3, 809 [arXiv:1304.1867 [hep-ph]]; Phys. Lett. B **704** (2011) 566 [arXiv:1101.6012 [hep-ph]]l Phys. Rev. Lett. **106** (2011) 142002 [arXiv:1101.0585 [hep-ph]].
[39] P.D.B. Collins, *"An introduction to Regge theory and high energy physics"*, Cambridge University Press 1977.
[40] A. H. Mueller, *Phys. Rev.* **D2** (1970) 2963.
[41] V. Khachatryan *et al.* [CMS Collaboration], JHEP **1009** (2010) 091 [arXiv:1009.4122 [hep-ex]].
[42] J. Adams *et al.* [STAR Collaboration], Phys. Rev. Lett. **95** (2005) 152301 [nucl-ex/0501016].
[43] B. Alver *et al.* [PHOBOS Collaboration], Phys. Rev. Lett. **104** (2010) 062301 [arXiv:0903.2811 [nucl-ex]].
[44] H. Agakishiev *et al.* [STAR Collaboration], arXiv:1010.0690 [nucl-ex].
[45] S. Chatrchyan *et al.* [CMS Collaboration], Phys. Lett. B **718** (2013) 795 [arXiv:1210.5482 [nucl-ex]].
[46] S. Chatrchyan *et al.* [CMS Collaboration], Eur. Phys. J. C **72** (2012) 2012 [arXiv:1201.3158 [nucl-ex]].
[47] A. Dumitru, F. Gelis, L. McLerran and R. Venugopalan, Nucl. Phys. A **810** (2008) 91 [arXiv:0804.3858 [hep-ph]].
[48] E. V. Shuryak, Phys. Rev. C **76** (2007) 047901 [arXiv:0706.3531 [nucl-th]]; S. A. Voloshin, Phys. Lett. B **632** (2006) 490 [nucl-th/0312065]; S. Gavin, L. McLerran and G. Moschelli, Phys. Rev. C **79** (2009) 051902 [arXiv:0806.4718 [nucl-th]].
[49] A. Kovner, *"How to build a ridge in pA collisions"*, talk at Low x WS, May 30 - June 4, 2013,Rehovot-Eilat, Israel. $http://www.weizmann.ac.il/MaKaC/getFile.py/access?contribId=60\&sessionId=25\&resId=0\&materialId=slides\&confId=16$
[50] A. Dumitru, K. Dusling, F. Gelis, J. Jalilian-Marian, T. Lappi and R. Venugopalan, Phys. Lett. B **697** (2011) 21 [arXiv:1009.5295 [hep-ph]].
[51] A. Kovner and M. Lublinsky, Phys. Rev. D **83** (2011) 034017 [arXiv:1012.3398 [hep-ph]].
[52] A. Kovner and M. Lublinsky, Int. J. Mod. Phys. E **22** (2013) 1330001 [arXiv:1211.1928 [hep-ph]].
[53] W. Li, Mod. Phys. Lett. A **27** (2012) 1230018 [arXiv:1206.0148 [nucl-ex]].
[54] A. Kovner, Acta Phys. Polon. B **42** (2011) 2717.
[55] C. J. Horowitz, Int. J. Mod. Phys. E **20** (2011) 1 [arXiv:1106.1661 [astro-ph.SR]].
[56] T. Lappi, Int. J. Mod. Phys. E **20** (2011) 1 [arXiv:1003.1852 [hep-ph]].
[57] E. Iancu, arXiv:1205.0579 [hep-ph].
[58] R. Venugopalan, PoS QNP **2012** (2012) 019 [arXiv:1208.5731 [hep-ph]].
[59] A. H. Mueller and B. Patel, Nucl. Phys. **B425** (1994) 471. A. H. Mueller and G. P. Salam, Nucl. Phys. **B475**, (1996) 293. [arXiv:hep-ph/9605302]. G. P. Salam, Nucl. Phys. **B461** (1996) 512; E. Iancu and A. H. Mueller, Nucl. Phys. **A730** (2004) 460 [arXiv:hep-ph/0308315]; 494 [arXiv:hep-ph/0309276].
[60] A. H. Mueller and D. N. Triantafyllopoulos, *Nucl. Phys.* **B640** (2002) 331 [arXiv:hep-ph/0205167];
[61] M. L. Good and W. D. Walker, Phys. Rev. 120 (1960) 1857.
[62] S. Munier and R. B. Peschanski, Phys. Rev. D **70** (2004) 077503 [arXiv:hep-ph/0401215]; Phys. Rev. D **69** (2004) 034008 [arXiv:hep-ph/0310357]; Phys. Rev. Lett. **91** (2003) 232001 [arXiv:hep-ph/0309177].
[63] H. Navelet and R. B. Peschanski, Nucl. Phys. **B 507**, 35 (1997) [hep-ph/9703238]; Phys. Rev. Lett. **82** (1999) 1370

[hep-ph/9809474]; Nucl. Phys. B **634** (2002) 291 [hep-ph/0201285].
[64] I. Gradstein and I. Ryzhik, *Table of Integrals, Series, and Products*, Fifth Edition, Academic Press, London, 1994.
[65] E. Iancu, K. Itakura and S. Munier, Phys. Lett. B **590**, 199 (2004) [hep-ph/0310338].
[66] S. Catani, M. Ciafaloni and F. Hautmann, Nucl. Phys. B **366** (1991) 135; Nucl. Phys. Proc. Suppl. 29A (1992) 182; J. C. Collins and R. K. Ellis, Nucl. Phys. B **360** (1991) 3; E. M. Levin, M. G. Ryskin, Y. .M. Shabelski and A. G. Shuvaev, Sov. J. Nucl. Phys. **53** (1991) 657 [Yad. Fiz. **53** (1991) 1059].
[67] Y. V. Kovchegov and K. Tuchin, Phys. Rev. **D65** (2002) 074026 [arXiv:hep-ph/0111362].
[68] G. Aad *et al.* [ATLAS Collaboration], New J. Phys. **15** (2013) 033038 [arXiv:1301.6872 [hep-ex]], V. M. Abazov *et al.* [D0 Collaboration], Phys. Rev. D **81** (2010) 052012 [arXiv:0912.5104 [hep-ex]], F. Abe *et al.* [CDF Collaboration], Phys. Rev. D **47** (1993) 4857, Phys. Rev. D **56** (1997) 3811, J. Alitti *et al.* [UA2 Collaboration], Phys. Lett. B **268** (1991) 145, T. Akesson *et al.* [Axial Field Spectrometer Collaboration], Z. Phys. C **34**, 163 (1987).
[69] Z. Koba, H. B. Nielsen, and P. Olesen, Nucl. Phys. B40 (1972) 317.
[70] E. Avsar, C. Flensburg, Y. Hatta, J. Y. Ollitrault and T. Ueda, Phys. Lett. B **702**, 394 (2011) doi:10.1016/j.physletb.2011.07.031 [arXiv:1009.5643 [hep-ph]].
[71] V. Khachatryan *et al.* [CMS Collaboration], JHEP **1009** (2010) 091 doi:10.1007/JHEP09(2010)091 [arXiv:1009.4122 [hep-ex]].
[72] G. Aad *et al.* [ATLAS Collaboration], *"Observation of long-range elliptic anisotropies in $\sqrt{s}$ =13 and 2.76 TeV pp collisions with the ATLAS detector,"* arXiv:1509.04776 [hep-ex].
[73] D. Kharzeev, E. Levin and L. McLerran, Nucl. Phys. A **748** (2005) 627, [hep-ph/0403271].
[74] We use the classification and terminology suggested in Ref. [49].

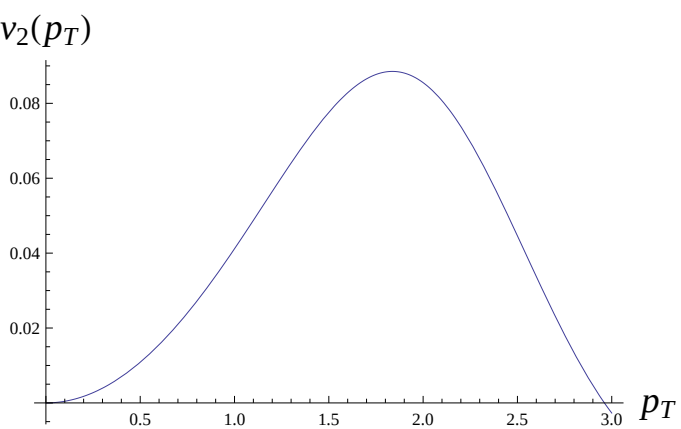
$v_2(p_T)$
0.08
0.06
0.04
0.02
0.5
1.0
1.5
2.0
2.5
3.0
p_T